Graphitic Carbon Nitride Functionalized Nickel-Cerium Bimetallic Oxide for Ultrasensitive Detection of Trichlorfon

A DISSERTATION

SUBMITTED IN PARTIAL FULFILLMENT OF THE REQUIREMENTS FOR THE AWARD OF THE DEGREE

OF

MASTERS OF SCIENCE

IN

(CHEMISTRY)

Submitted by

Akanksha Katoch
(2K24/MSCCHE/62)

And

Komal
(2K24/MSCCHE/33)

Under the Supervision of

Prof. D. Kumar

DEPARTMENT OF APPLIED CHEMISTRY
DELHI TECHNOLOGICAL UNIVERSITY
(Formerly Delhi College of Engineering)
Shahbad Daulatpur Bawana Road, Delhi -110042

JUNE, 2026

DELHI TECHNOLOGICAL UNIVERSITY
(Formerly Delhi College of Engineering)
Shahbad Daulatpur, Main Bawana Road, Delhi -110042

CANDIDATE'S DECLARATION

We, **Akanksha Katoch (2K24/MSCCHE/62)** and **Komal (2K24/MSCCHE/33)** of **M.Sc. (Applied Chemistry)**, hereby declare that the Project Dissertation titled "**Graphitic Carbon Nitride Functionalized Nickel-Cerium Bimetallic Oxide for Ultrasensitive Detection of Trichlorfon**" which is submitted by us to the Department of Applied Chemistry, Delhi Technological University in partial fulfillment of the requirements for the award of the Degree of Master of Science in Chemistry, is original and not copied from any source without proper citation. This work has not previously formed the basis for the award of any degree, diploma associateship, fellowship or other similar title or recognition.

Akanksha Katoch
(2K24/MSCCHE/62)

Komal
(2K24/MSCCHE/33)

Place: Delhi

Date: 22/06/2026

Department of Applied Chemistry
DELHI TECHNOLOGICAL UNIVERSITY
(Formerly Delhi College of Engineering)
Shahbad Daulatpur, Main Bawana Road,
Delhi -110042

CERTIFICATE

We hereby certify that Project Dissertation titled **"Graphitic Carbon Nitride Functionalized Nickel-Cerium Bimetallic Oxide for Ultrasensitive Detection of Trichlorfon"** which is submitted by **Akanksha Katoch (2K24/MSCCHE/62)** and **Komal (2K24/MSCCHE/33), Department of Applied of Chemistry, Delhi Technological University** in partial fulfillment of the requirements for the award of the Degree of Master of Science in Chemistry, is a record of the project work carried out by the student under my supervision. To the best of my knowledge this work has not been submitted in part or full for any degree or diploma to this university or elsewhere.

Prof. D. Kumar
(Supervisor)

Place: Delhi

Date: 22/06/2026

ABSTRACT

Organophosphate pesticides are widely used in agriculture to protect crops from pest damage; however, excessive use contaminates soil, water, and food products, posing serious environmental and health risks. Trichlorfon (TF), an organophosphate pesticide, strongly inhibits the enzyme acetylcholinesterase (AChE), disrupting the nervous system. Therefore, the development of a rapid and sensitive method for TF detection is highly important to food safety and environmental monitoring. In this study, we report the fabrication of an electrochemical biosensor based on AChE immobilized on a Ce-NiO@g-C_3N_4 nanocomposite-modified indium tin oxide (ITO) electrode for ultrasensitive detection of TF. The Ce-NiO@g-C_3N_4 nanocomposite provides excellent electrical conductivity, large surface area, enhanced electron transfer, and superior electrocatalytic activity, which facilitate efficient enzyme immobilization and improve sensing performance. Glutaraldehyde was used as a crosslinking agent to enhance enzyme stability and prevent leaching from the electrode surface. The fabricated AChE/Ce-NiO@g-C_3N_4/ITO biosensor exhibited high sensitivity (5.412 $\mu A \mu M^{-1} cm^{-2}$), excellent stability, good reproducibility, and strong anti-interference capability for TF detection over a wide linear range, with a low detection limit of 0.1 pM. Furthermore, the developed biosensor was successfully applied to the determination of trichlorfon residues in real agricultural samples, including apple, cucumber, and rice, demonstrating satisfactory recovery and practical applicability. The proposed biosensor offers a simple, rapid, cost-effective, and highly efficient platform for monitoring organophosphate pesticides in food and environmental samples.

DELHI TECHNOLOGICAL UNIVERSITY
(Formerly Delhi College of Engineering)
Shahbad Daulatpur, Main Bawana Road,
Delhi -110042

ACKNOWLEDGEMENT

Firstly, we would like to express our deepest gratitude to our supervisor and Head Prof. D. Kumar, Department of Applied Chemistry, Delhi Technological University, Delhi, for his continuous support, guidance, and encouragement throughout our M.Sc. journey. His expertise, insightful feedback, and patience were invaluable in the successful completion of this thesis.

We are really grateful to Prof. Ram Singh for providing the facilities required for our research.

We were privileged to work in a supportive laboratory environment, and we appreciate the cooperation of our batchmates and research scholars. We would especially like to thank Dr. Divya Hudda for her invaluable assistance in teaching us the basic concepts of methods and for her patience in answering all our queries during our research. We are also thankful to Ms. Tanushee for her support of our project. We warmly acknowledge the entire faculty of the Department of Applied Chemistry at DTU for their constant support and cooperation. Furthermore, we would like to thank the technical and non-technical staff for their help when required.

Last, we are immensely grateful to our family and friends for their encouragement, support, and motivation throughout this journey.

Akanksha Katoch **(2K24/MSCCHE/62)**

Komal **(2K24/MSCCHE/33)**

DELHI TECHNOLOGICAL UNIVERSITY

(Formerly Delhi College of Engineering)
Shahbad Daulatpur, Main Bawana Road, Delhi- 42

PLAGIARISM VERIFICATION

Title of thesis: "**Graphitic Carbon Nitride Functionalized Nickel-Cerium Bimetallic Oxide for Ultrasensitive Detection of Trichlorfon**".

This is to report that the above thesis was scanned for similarity detection. Process and outcome are given below:

Software used: **Turnitin**

Similarity Index: **8 %**

Total Word Count: **22560**

Date: 22/06/2026

Akanksha Katoch	**Komal**	**Prof. D Kumar**
(2K23/MSCCHE/62)	**(2K23/MSCCHE/33)**	**(Supervisor)**

CONTENTS

LIST OF FIGURES

LIST OF TABLES

ABBREVIATIONS

OPP	Organophosphorus Pesticide
g-C_3N_4	Graphitic Carbon Nitride
$Ti_3C_2T_X$	MXene
AChE	Acetylcholinesterase
ATCl	Acetyl thiocholine chloride
TF	Trichlorfon
ITO	Indium tin oxide
EPD	Electrophoretic Deposition
XRD	X-Ray Diffraction
FT-IR	Fourier Transform Infrared
FESEM	Field Emission Scanning Electron Microscope
EDX	Energy Dispersive X-Ray Spectroscopy
PBS	Phosphate Buffer Saline
CV	Cyclic Voltammetry
DPV	Differential Pulse Voltammetry
EIS	Electrochemical impedance spectroscopy
RSD	Relative Standard Deviation
LOD	Limit of detection

Chapter – 1

Introduction

1. Introduction to Pesticides

The word pesticide is derived from the Latin words *pestis, meaning plague, and caedere,* meaning kill. Pesticides are chemical or biological agents used to protect crops and the environment by preventing, repelling, destroying, or controlling pests such as insects, rodents, fungi, and weeds. Pesticides serve as plant protection products because they protect from insects, rodents, nematodes or weeds. The Food and Agriculture Organization (FAO) has defined *pesticide* as:

"Any substance or mixture of substances intended for preventing, destroying, or controlling any pest, including vectors of human or animal disease, unwanted species of plants or animals, causing harm during or otherwise interfering with the production, processing, storage, transport, or marketing of food, agricultural commodities, wood and wood products or animal feedstuffs, or substances that may be administered to animals for the control of insects, arachnids, or other pests in or on their bodies. The term includes substances intended for use as a plant growth regulator, defoliant, desiccant, or agent for thinning fruit or preventing the premature fall of fruit. Also used as substances applied to crops either before or after harvest to protect the commodity from deterioration during storage and transport".

1.1 Categories of Pesticides

Pesticides can be classified in different ways according to:

1. Their source
2. Their target
3. Their mode of action
4. Their chemical structure

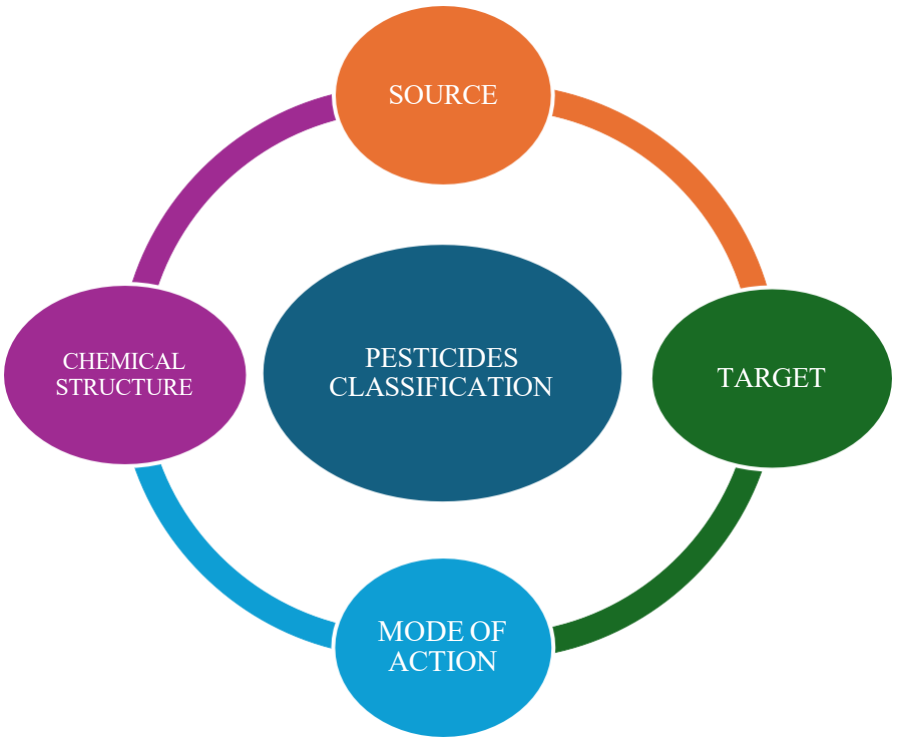

Fig. 1.1 Classification of pesticides

1.1.1 Based on the Sources

- Natural Pesticides: Natural pesticides are derived from naturally available resources, including plant extracts and mineral compounds, and are used for effective pest management. Nicotine, rotenone, pyrethrum, and neem oil are examples of natural pesticides derived from plants. Boric acid, used to control pests such as termites and cockroaches, is a mineral. Diatomaceous earth is a dry powdery material derived from the shells of marine organisms. It is used mainly to deter and kill crawling pests.
- Synthetic Pesticides: Synthetic pesticides are man-made chemicals such as DDT, malathion, dieldrin, and carbofuran that are designed to kill or repel pests in agriculture and homes. The use of synthetic pesticides began in the 1930's. The first known pesticide is arsenic, and the most popular one has been DDT (Dichloro Diphenyl Trichloroethane), which was introduced in 1934 by the scientist Paul Muller during World War II. It was an effective tool for eradicating malaria. By 1950, pesticides were found to increase farm yields.

Farmers worldwide today primarily rely on synthetic pesticides to control pests in their crops. As India is a tropical country, it suffers severe agricultural losses due to pests. This necessitates the use of pesticides to protect crops from multiple pests. Today, pesticides have become an evil necessity we cannot do without. Even though they are poisonous chemicals, they are a major saviour of humankind, as they help us meet the increasing demands of a growing population.

1.1.2 Based on the Targets

- Insecticides: Insecticides constitute a class of pesticides that are intended to prevent, control, or eradicate harmful insects.
- Herbicides: Herbicides are used to kill desirable plants or weeds.
- Fungicides: Fungicides are chemicals that are applied to prevent, manage, and eradicate fungal diseases that develop on fruits, vegetables, and cereal crops.
- Rodenticides: Rodenticides are chemical compounds that are used against rodents such as rats and mice.
- Nematicides: Nematicides are chemical pesticides that are used to kill plant-parasitic nematodes. Nematodes are parasitic worms that live in soil and feed on living material.

1.1.3. Based on their Action

- Stomach poisons: Insecticides taken up by insects are called stomach poisons. E.g. BHC, DDT, lead arsenate.
- Contact poisons: The insecticides that destroy the insects simply by body contact. E.g. BHC, aldrin, malathion.
- Fumigants: The insecticides that act on the insect through the respiratory system. E.g. BHC, HCN, nicotine.
- Systematic pesticides: The pesticides that are absorbed by the roots, stems and leaves of the plant. When insects feed on these areas of the plant, they are killed.

1.1.4 Based on the Chemical Structure

- Organochlorines: Organochlorine pesticides are chlorinated hydrocarbons. These are used in agriculture and mosquito control. Some important organochlorine pesticides include DDT and BHC.

- Organophosphates: Organophosphates are esters of phosphoric acid, thiophosphoric acid and dithiophosphoric acid. These are used in agriculture, in gardens and lawns. Commonly used organophosphates include parathion, malathion, and diazinon.

a. Carbamates: Carbamates are esters of carbamic acid (NH_2COOH). Examples of carbamates include carbaryl and methiocarb.
b. Quinones: Quinone pesticides are derivatives of benzoquinone. They act as fungicides. Examples are chloranil, dichlone, and dithianon.
c. Anilides: Anilide pesticides are the acyl derivatives of aniline. These are herbicides in action, used to control weed growth in crops. The anilides include alachlor, butachlor, propanil, and acetochlor.

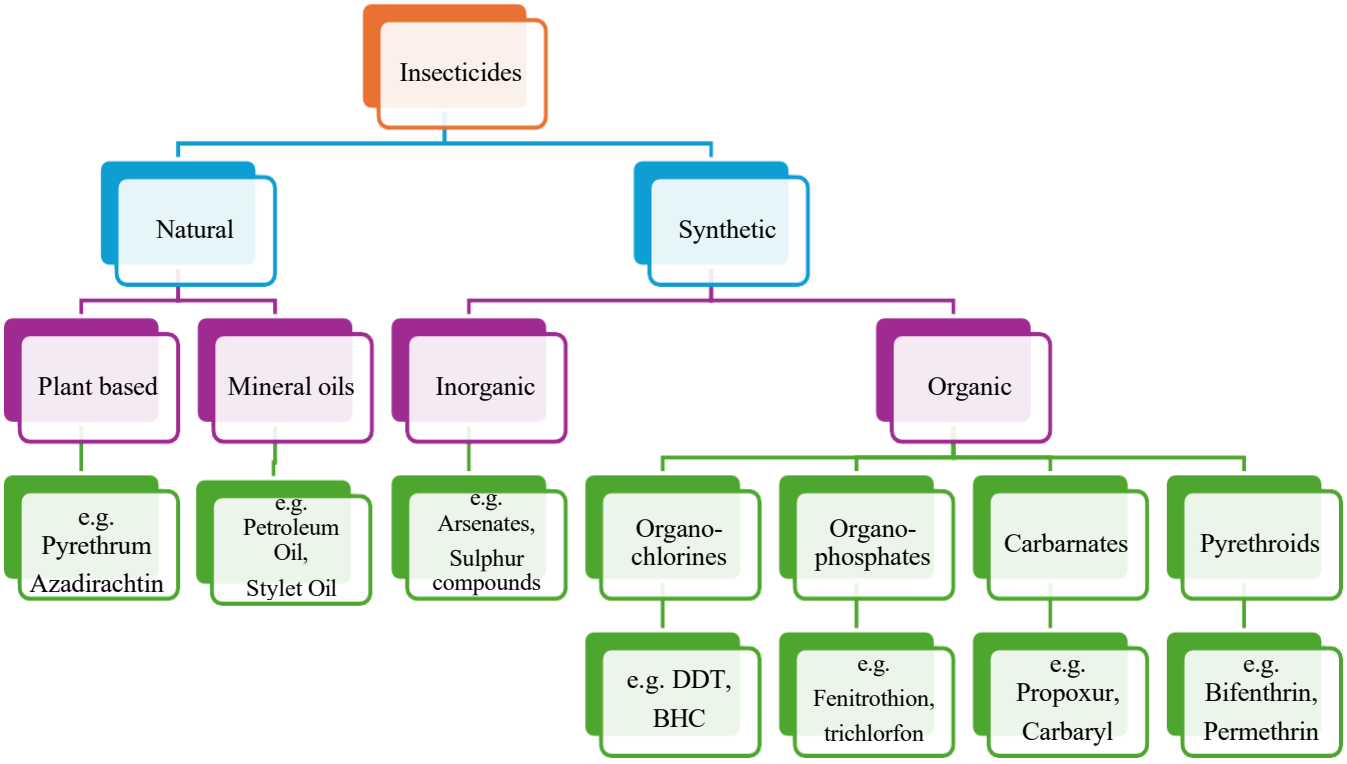

Fig. 1.2 Classification of Insecticides

1.2 Benefits of Pesticides

The primary objective of agriculture is to produce crops and livestock for human use. With the continuous growth of the World's population, ensuring an adequate food supply has become increasingly important. However, many insects, weeds, fungi, and other organisms also utilize these crops as a food source, leading to significant agricultural losses. To avoid significant food losses, pesticides are often needed to address the problem.

Regardless of the negative, hazardous effects of pesticides, they have become a necessary evil in today's world, and we cannot completely ban them. However, we can shift to safer and less toxic alternatives. The benefits of pesticides are as follows:

- Improving productivity: The adoption of pesticides has played a vital role in modern agriculture by improving crop production and reducing yield losses caused by weeds, insect pests, and plant diseases. Their use enables farmers to optimize the performance of complementary agricultural inputs, such as improved seed varieties, fertilizers, advanced irrigation methods, and other crop management practices. Consequently, pesticides have contributed substantially to enhanced productivity and more efficient utilization of agricultural land, thereby potentially increasing the harvestable produce. Farmers can increase profits and reduce labour costs.
- Reducing waterborne and insect-transmitted diseases: Pesticides play an important role in protecting public health by controlling insects and rodents that act as carriers of infectious diseases. Reducing the populations of these disease vectors helps limit the spread of vector-borne illnesses. In many situations, insecticides remain among the most effective and practical methods for managing insects that transmit diseases such as malaria and West Nile virus.
- Conservation of the environment: Pesticides enable the use of pesticides enhances agricultural productivity by enabling greater crop production per unit area and improving the efficient use of farming resources. Higher yields help reduce pressure to expand land, thereby limiting deforestation, conserving natural ecosystems, and preventing soil degradation. Furthermore, pesticides are essential for controlling invasive pests and noxious weeds that adversely affect crop production.
- In many developing countries, crop protection technologies have supported food security by increasing crop yields and encouraging the cultivation of diverse agricultural commodities, so much so that these countries now have the capacity to export their food.
- Help in storage: After the crop has been cut and is put in storage, it can still be subjected to pest attacks. Bugs, rodents, and moulds can harm the storage.

1.3 Adverse Effects of Pesticides

Pesticides have been linked to a wide range of hazards, including health hazards and environmental hazards. In India, 65% of pesticide use is in the agricultural sector, with the remainder in the non-agricultural sector. While pesticides have played an important role in increasing agricultural productivity and improving farmers' economic returns, their benefits are accompanied by significant environmental and health concerns. Continuous and excessive pesticide application can

contaminate soil, water, and agricultural produce. Residual pesticides may enter the food chain and accumulate in living organisms, posing potential health risks to humans. Furthermore, these chemicals can unintentionally harm non-target plants, beneficial insects, aquatic organisms, birds, and other wildlife, thereby disrupting ecological balance and reducing biodiversity.

- **Health Hazard:** Pesticides are recognized as an important source of chemical exposure that can adversely affect human health. The severity of these effects depends on factors such as the type of pesticide, duration of exposure, concentration, and route of entry into the body. Acute exposure is commonly associated with symptoms including headache, dizziness, nausea, vomiting, skin irritation, and eye irritation. Numerous epidemiological and toxicological investigations have suggested a relationship between long-term pesticide exposure and an increased prevalence of neurological disorders, particularly Parkinson's disease, as well as haematological malignancies such as lymphoma and leukaemia. Respiratory illnesses, including asthma, have also been reported more frequently among individuals with regular pesticide exposure. Occupational exposure represents one of the primary routes through which individuals come into contact with pesticides. Workers engaged in pesticide manufacturing, formulation, packaging, transportation, mixing, loading, spraying, and agricultural application are at greater risk of exposure than the general population. Organochlorine pesticides are particularly concerning because of their exceptional environmental persistence and lipophilic nature. These compounds degrade slowly and readily accumulate in fatty tissues of living organisms. Once released into the environment, they can be transported by air, soil, and water, contaminating terrestrial and aquatic ecosystems across large geographic areas.
- **Environmental Impact:** The extensive application of pesticides has raised significant environmental concerns due to their widespread distribution beyond the intended target areas. After application, pesticide residues may contaminate soil, surface water, groundwater, and surrounding vegetation through processes such as runoff, leaching, spray drift, and volatilization. Although these chemicals are primarily designed to control agricultural pests and weeds, they can also adversely affect numerous non-target organisms, including beneficial insects, birds, aquatic animals, soil microorganisms, and native plant species. A considerable proportion of applied pesticides fails to reach the target pest. Instead, they disperse into the surrounding environment, where they may persist for varying periods depending on their chemical properties and environmental conditions. Many pesticides are resistant to degradation and can remain in soil, water, and the atmosphere long after their initial application.
- **Surface Water Contamination:** The contamination of water resources by pesticides has emerged as a significant environmental issue resulting from intensive agricultural practices. After

application, these chemicals may be transported from cultivated fields into nearby rivers, lakes, ponds, and reservoirs through rainfall-induced runoff or irrigation. Pesticides may also enter water bodies via spray drift, leaching through the soil profile, seepage into groundwater, drainage systems, or accidental spills during handling and application. Their presence in aquatic environments can degrade water quality, threaten aquatic biodiversity, and pose health hazards to humans who rely on these waters for drinking and domestic use.

- **Groundwater Contamination:** Groundwater is particularly vulnerable to pesticide pollution because many pesticide molecules can migrate downward through soil and reach underground aquifers. The extent of contamination depends on several factors, including soil characteristics, rainfall patterns, irrigation practices, and the pesticide's persistence. Monitoring studies conducted across different agricultural regions have detected measurable concentrations of pesticide residues, including persistent organochlorine compounds, in drinking water. Since groundwater moves slowly and natural purification processes are limited, contaminated aquifers often require many years or even decades for recovery, making groundwater pollution a serious environmental and public health concern.
- **Soil Contamination:** Long-term application of pesticides can substantially influence soil quality by altering its biological and chemical properties. Several pesticides are resistant to natural degradation, allowing them to accumulate in soil over extended periods. Persistent residues can suppress beneficial microbial populations that play essential roles in nutrient cycling, organic matter decomposition, and the maintenance of soil fertility. A reduction in microbial diversity and activity ultimately weakens soil health, decreases agricultural sustainability, and limits the productive capacity of cultivated land.
- **Effects on Plants:** In addition to controlling weeds and pests, pesticides may unintentionally interfere with normal plant growth and development. Some pesticide compounds disrupt the symbiotic relationship between legumes and nitrogen-fixing bacteria, thereby reducing the availability of biologically fixed nitrogen required for healthy plant growth. Excessive pesticide exposure may also impair root development, reduce chlorophyll content, inhibit photosynthesis, and slow overall plant growth. Furthermore, pesticide-induced declines in pollinator populations, particularly bees and other beneficial insects, reduce pollination efficiency, resulting in reduced crop yields and lower reproductive success in flowering plants.
- **Effects on Animals:** The widespread use of pesticides poses considerable risks to both domestic and wild animal populations. Exposure may occur through contaminated food, water, soil, or direct contact with treated vegetation. Because many pesticides persist in the environment, toxic residues can accumulate within animal tissues and become increasingly concentrated at higher trophic

levels through biomagnification. Such exposure may lead to behavioural changes, reproductive disorders, developmental abnormalities, immune suppression, and increased mortality in wildlife. Pesticide contamination can also reduce the abundance of insects and other organisms that serve as important food sources, thereby disturbing ecological food webs. In humans, health outcomes depend on pesticide toxicity and the degree of exposure. Reported effects include skin and eye irritation, respiratory disorders, neurological impairment, endocrine disruption, reproductive toxicity, congenital abnormalities, genetic damage, various forms of cancer, and, under severe exposure conditions, coma or death.

1.4 Sustainable and Eco-Friendly Alternatives to Chemical Pesticides

The primary purpose of pesticide application is to minimize crop losses caused by insects, weeds, plant pathogens, and other harmful organisms, thereby enhancing agricultural yield and ensuring food quality. In addition to their role in crop protection, pesticides are important in public health programs for controlling vectors that spread infectious diseases, including malaria and dengue. Their use is not limited to agricultural systems; various classes of pesticides, such as insecticides, herbicides, fungicides, and rodenticides, are also applied in non-agricultural settings. These include parks, recreational grounds, sports facilities, lawns, and other urban landscapes, where they help manage unwanted vegetation, insects, fungi, and rodents to maintain environmental hygiene, aesthetics, and public safety.

Numerous dermatological, gastrointestinal, reproductive, respiratory and carcinogenic effects have been associated with pesticides. Pesticide residues have been found in everyday foods, beverages, water, and animal feeds. Pesticides have been detected in human breast milk, which can have health effects in children.

The adverse effects of pesticides on wildlife and aquatic life are alarming. It is evident that the use of chemical pesticides also poses the risk of severe environmental pollution. In this situation, there is an urgent need for a new approach to pesticide use.

Need for Cleaner, Safer Agricultural Practices: Current agricultural practices rely heavily on pesticides, which are known to cause adverse health effects in humans and wildlife. These chemicals also degrade the natural environment. Therefore, an urgent approach is needed to drastically reduce the use of agrochemicals. Agrochemicals should be applied only when and where necessary. Factors such as yield, soil type, crop, wind damage, and flooding must be taken into consideration before applying pesticides. The use of innovative technological systems, such as geographical information systems, various sensors, and global positioning systems, can help

reduce pesticide use.

Suitable Agricultural Practices: Suitable agricultural practices can produce healthy crops and prevent the buildup of pests, diseases, and weeds. As a result, the need for pesticides is reduced. The following practices should be employed:

- The use of organic matter for plant nutrition and soil fertility reduces pest, disease, and weed attacks.
- Crop rotation prevents the carry-over of pests, pathogens and weeds.
- The cultivation of two or more crops in the same field can suppress the movement and establishment of pests and pathogens while creating a favorable environment for beneficial insects that naturally regulate pest populations.
- Suitable irrigation management reduces the proliferation of pests and weeds.
- Sowing or planting at the appropriate time reduces pest pressure.

Resistant Crops: Growing crops suited to local conditions and selecting appropriate crop varieties are very important for preventing pest growth. The genetically engineered crops are more resistant. So, the use of resistant varieties, together with crop rotation, can greatly reduce pest populations in the fields.

Bio-Control: In bio-control, various pathogens (bacteria, fungi, viruses), insect predators, pheromones, and insect traps are employed to keep pest populations low. The most commonly used bio-control methods are:

- Release of pest predators in the fields, such as Trichogramma and ladybirds.
- Application of biological control agents, including beneficial microorganisms such as *Bacillus thuringiensis*, *Beauveria* spp., *Trichoderma* spp., and entomopathogenic nematodes, can effectively suppress pest populations by infecting or inhibiting target organisms.
- The use of pheromone-based technologies provides an environmentally friendly approach to pest management by interfering with insect communication and mating behavior, thereby reducing successful reproduction and limiting population growth.

Natural Pesticides: Various plant extracts and other natural materials are used to repel pests. Most commonly used natural pesticides are:

- The neem seed extract reduces the proliferation of insect pests.
- Pyrethrum, the extract of Chrysanthemum species, promotes beneficial insects.
- Copper is widely used to control fungal diseases.
- Sulphur, soap and paraffinic oil preparations are used to control mites, aphids and other pests.

Organic Agriculture: Organic agriculture is an environmentally sustainable production system that aims to preserve soil fertility, ecological balance, and human well-being by avoiding the use of synthetic agrochemicals. Rather than relying on chemical pesticides, it integrates ecological principles and preventive management practices to minimize pest and disease incidence. Techniques such as crop diversification, crop rotation, intercropping, incorporation of organic fertilizers, cultivation of pest-resistant cultivars, and the use of biological control organisms are widely adopted to maintain healthy crop production. In situations where pest intervention is necessary, only naturally derived or organically approved plant protection products are permitted to minimize impact on the environment and non-target organisms.

Adoption of Safer Pesticides: Reducing the environmental and health risks associated with pesticide use can also be achieved by encouraging the adoption of lower-toxicity, more environmentally compatible pesticides. Replacing highly hazardous compounds with safer alternatives decreases the likelihood of adverse effects on farmers, consumers, beneficial organisms, and wildlife. In addition, selecting pesticides that degrade more rapidly and exhibit lower persistence in the environment helps reduce contamination of soil and water resources while maintaining satisfactory pest control. The use of such safer formulations represents an important component of integrated and sustainable pest management strategies [1].

1.5 Biosensors

"A biosensor is an analytical device designed to recognize biological events and translate them into measurable electrical signals. It works by integrating a biological recognition component with a signal-converting transducer and is widely used in fields such as medical diagnosis and environmental analysis" [2]. These instruments are widely used to detect and quantify biologically significant substances. Even when the sensor does not directly interface with a living biological system, it can still detect biologically meaningful parameters [3]. This device uses a biorecognition element, such as an enzyme, antibody, or nucleic acid, to specifically bind with the analyte of interest, enabling its detection and quantification [4]. This biological interaction produces a response that is converted into an electrical signal by a transducer. Depending on their intended use,

biosensors can be categorized into various types, including immunosensors, resonant mirror sensors, chemical canaries, biocomputers, glucometers, and biochips [5]. Broadly, a biosensor is defined as an analytical system integrating a biological recognition element with a signal transducer to produce qualitative or semi-quantitative results. In essence, biosensors monitor variations in biological activity and convert these changes into electrical outputs, enabling their use in diverse fields such as healthcare diagnostics, environmental analysis, and industrial applications [6].

Compared with many conventional diagnostic tools, biosensors offer superior selectivity and sensitivity [7]. They are widely used in environmental pollution monitoring, agriculture, and the food industry. Important characteristics of biosensors include good stability, affordability, and high sensitivity [8].

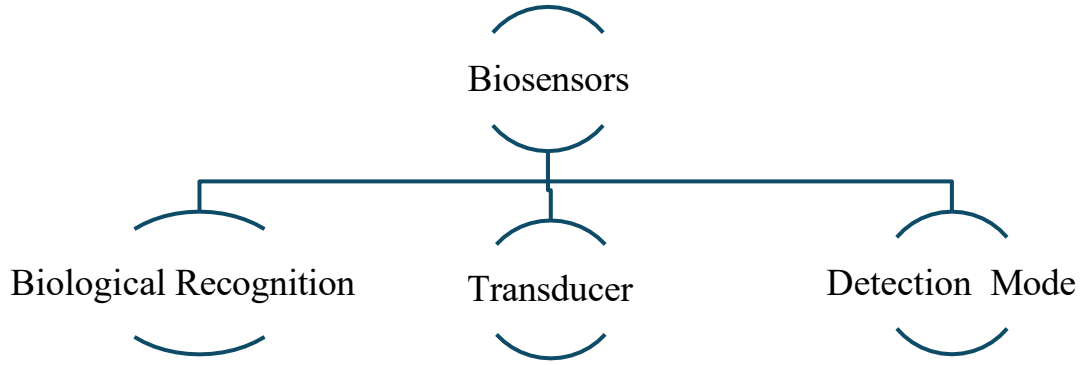

Fig. 1.3 Classification of Biosensors

1.5.1 Components of Biosensors

Biosensors are analytical devices composed of multiple interconnected components, each playing an important role in detecting and measuring biological or chemical substances. The proper functioning of these elements ensures high accuracy, sensitivity, and reliability [9]. The major components of a biosensor are explained below in an original and simplified manner [10].

The components of a biosensor are as follows:

1. **Analyte**

   The analyte is the substance being detected or measured by the biosensor. It can be a chemical compound, biological molecule, or microorganism present in a sample [11]. Common examples include glucose, enzymes, pollutants, toxins, or disease markers. Detection begins when the analyte comes into contact with the sensing system [12].

2. **Biological Recognition Element**

   This component is responsible for identifying the analyte with high specificity. It is typically made of biological materials such as enzymes, antibodies, DNA, RNA, microorganisms, or living cells. The recognition element selectively interacts with the target analyte and elicits a biological

response [13].

3. **Transducer**

   The transducer transforms the biological interaction into a measurable signal. This signal may be electrical, optical, thermal, or mechanical in nature [14]. Depending on the type of biosensor, transducers can be electrochemical, optical, piezoelectric, or thermal. This conversion allows quantification of the biological event [15].

4. **Signal Processing Unit**

   The signal generated by the transducer is often weak and requires enhancement. The signal processing unit amplifies, filters, and converts the signal into a usable format. It ensures that the output data is accurate and easy to interpret [16].

5. **Output and Display System**

   This component presents the processed signal in a readable form, such as numerical values, graphs, or visual indicators [17]. It enables users to clearly and quickly assess the presence or concentration of the analyte [18].

6. **Support Structure and Immobilization System**

   The support structure holds the biological element securely in place while maintaining its activity and stability. It also protects the biosensor's internal components from environmental factors, thereby improving its durability and performance [19].

   Together, these components enable biosensors to provide rapid, accurate, and reliable detection, which has led to their extensive use in healthcare, environmental analysis, and food safety monitoring and industrial applications [20,21].

1.5.2 Characteristics of a Biosensor

Biosensors are characterized by several performance-related features that determine how effectively they can detect and measure target substances in practical applications. A clear understanding of these characteristics is important for evaluating their usefulness in academic research, healthcare, industry, and environmental studies [22]. The main characteristics of biosensors are described below:

1. **Sensitivity**

   Sensitivity describes the capability of a biosensor to recognize very small quantities of an analyte. Sensors with high sensitivity can detect slight variations in concentration, which is essential for early disease identification, trace chemical analysis, and monitoring low-level biological processes [23]. Sensitivity is influenced by the nature of the biological sensing element and the efficiency of signal conversion [24].

2. **Selectivity (Specificity)**

Selectivity refers to the ability of a biosensor to respond only to the target analyte while ignoring other substances present in the sample [25]. This property depends mainly on the biological recognition element, which is designed to interact specifically with the analyte [26]. High selectivity helps reduce interference and improve measurement reliability [27].

3. **Accuracy**

Accuracy indicates how closely the results from a biosensor match the true analyte concentration [28]. Accurate sensors are essential in clinical diagnostics and quality control, where incorrect readings can lead to serious consequences [29].

4. **Response Time**

Response time is the time a biosensor takes to produce a stable output after contact with the analyte [30,31]. A short response time enables rapid detection and real-time monitoring, which are particularly useful in emergency medical care and continuous environmental assessment [32].

5. **Reproducibility**

Reproducibility is the ability of a biosensor to deliver consistent results when the same measurement is repeated under identical conditions. Good reproducibility reflects reliable sensor construction and stable biological activity [33].

6. **Stability**

Stability refers to a biosensor's ability to maintain consistent performance over long periods of use or storage. A stable biosensor continues to function effectively despite changes in temperature and pH, and withstands repeated measurements, making it suitable for long-term applications [34,35].

7. **Measurement Range**

The measurement range defines the analyte concentrations over which the biosensor can provide reliable results. A broader range increases the biosensor's flexibility, enabling its use in diverse analytical situations [36].

8. **Detection Limit**

The detection limit represents the lowest amount of analyte that the biosensor can reliably identify [37]. A lower detection limit indicates higher performance, which is important in applications such as toxin detection and early disease screening [38].

9. **Cost Efficiency**

Cost efficiency refers to the expenses associated with the biosensor's production, operation, and maintenance. Economical biosensors support large-scale manufacturing and make advanced detection technology more accessible [39].

10. **Portability and User Convenience**

Portability refers to the ease with which a biosensor can be carried and used outside laboratory environments [25,27]. Lightweight design, simple operation, and minimal power requirements make biosensors suitable for point-of-care testing and fieldwork [36].

11. **Biocompatibility**

Biocompatibility refers to a biosensor's ability to operate effectively without causing harmful effects when it comes into contact with biological systems. This feature is particularly important for wearable or implantable sensors used in continuous health monitoring [33,35].

12. **Reliability and Durability**

Reliability ensures that the biosensor produces dependable results over repeated use, while durability reflects its resistance to environmental and mechanical stress. These qualities are essential for practical and long-term deployment [34,32,40].

1.5.3 Working of a Biosensor

A biosensor is a device that detects biological or chemical substances and converts the resulting biological interaction into a measurable electrical signal. The operation of a biosensor involves a sequence of interconnected steps, from recognition of the target analyte to display of the final measurement [41]. Each step is crucial for achieving accuracy, sensitivity, and reliability in detection. The working mechanism can be described in the following detailed stages:

1. **Biological Recognition and Signal Transduction**

The heart of a biosensor lies in its biological recognition element. This component, which can be an enzyme, antibody, nucleic acid, or even whole cells, is specifically designed to interact with the target analyte. When the analyte contacts the recognition element, a biochemical reaction occurs.

For example, in a glucose biosensor, glucose reacts with the enzyme glucose oxidase, generating hydrogen peroxide as a byproduct [42].

This biochemical event creates a biological signal, often in the form of a chemical change (e.g., proton release, electron transfer, or a change in concentration of a reaction product). The transducer then converts this biochemical signal into an electrical form, such as a change in voltage, current, or impedance, which can be measured [43]. The choice of transducer (electrochemical, optical, piezoelectric, or thermal) depends on the reaction type and the desired sensitivity [44].

2. Signal Generation

The interaction between the target analyte and the biological recognition element is converted by the transducer into an electrical signal whose magnitude is directly proportional to the analyte concentration. For instance, in amperometric biosensors, the chemical reaction produces a current [45]. In potentiometric biosensors, a change in voltage occurs. If the output is a current, it may need to be converted to a voltage using a current-to-voltage converter based on an operational amplifier (Op-Amp). This ensures compatibility with subsequent electronic processing [46].

3. Characteristics of the Initial Signal

The raw electrical signal produced by the transducer is often very small and can be easily masked by noise. Noise may originate from environmental electromagnetic interference, thermal fluctuations in the components, or intrinsic variations in the sensor materials.

Without further processing, this low-level signal would be unreliable for accurate measurement. [47]

4. Signal Amplification

To make the signal usable, it is amplified using electronic circuits, often incorporating Op-Amps. Amplification increases the signal strength while preserving its proportionality to the analyte concentration [48]. This step is essential because it enables the sensor to detect very low analyte concentrations that would otherwise be lost in the noise.

5. Signal Filtering

Even after amplification, high-frequency noise or unwanted fluctuations may still interfere with the measurement. To eliminate this, the signal passes through a filter, commonly a low- pass RC (resistor-capacitor) filter. This filter allows low-frequency signals (which correspond to the actual

analyte concentration) to pass while removing high-frequency noise, producing a smooth and clear signal suitable for processing [49].

6. **Signal Processing and Conditioning**

The filtered signal is then sent to a signal processing or conditioning unit. Here, the signal may be further amplified, linearized, or corrected for temperature or environmental variations [50]. At this stage, the signal remains in analogue form, meaning it continuously varies in proportion to the analyte concentration. The conditioned analogue signal provides a direct representation of the biochemical interaction [51].

7. **Conversion to Digital Signal**

For easier display, data storage, and analysis, the analogue signal is usually converted into a digital format. This is performed by an analogue-to-digital converter (ADC) within a microcontroller or processor. The digital signal allows the biosensor to interface with computers, data loggers, or display devices, enabling further computational analysis, remote monitoring, or integration into automated systems [52].

8. **Output Display**

The final processed signal is presented to the user in an interpretable format, such as a numeric value on a digital screen, a graphical chart, or even a visual alarm if thresholds are exceeded. The output directly correlates to the concentration of the target analyte, providing actionable information for decision-making. For example, in medical applications, a glucose biosensor will display blood glucose levels in mg/dL, allowing immediate clinical evaluation [53].

Summary of the Process

In essence, the working of a biosensor involves:

Recognition: The analyte interacts with the biological element.

Transduction: The biological response is converted into an electrical signal.

Amplification & Filtering: The weak signal is amplified, and noise is filtered out.

Processing: The signal is conditioned, possibly converted to digital form.

Output: The measurement is displayed or recorded for interpretation

1.5.4 Types of Biosensors

Biosensors can be classified according to several criteria, such as the type of biological recognition element, the method of signal transduction, or their application. Each classification highlights the

unique way the biosensor operates and interacts with the analyte.

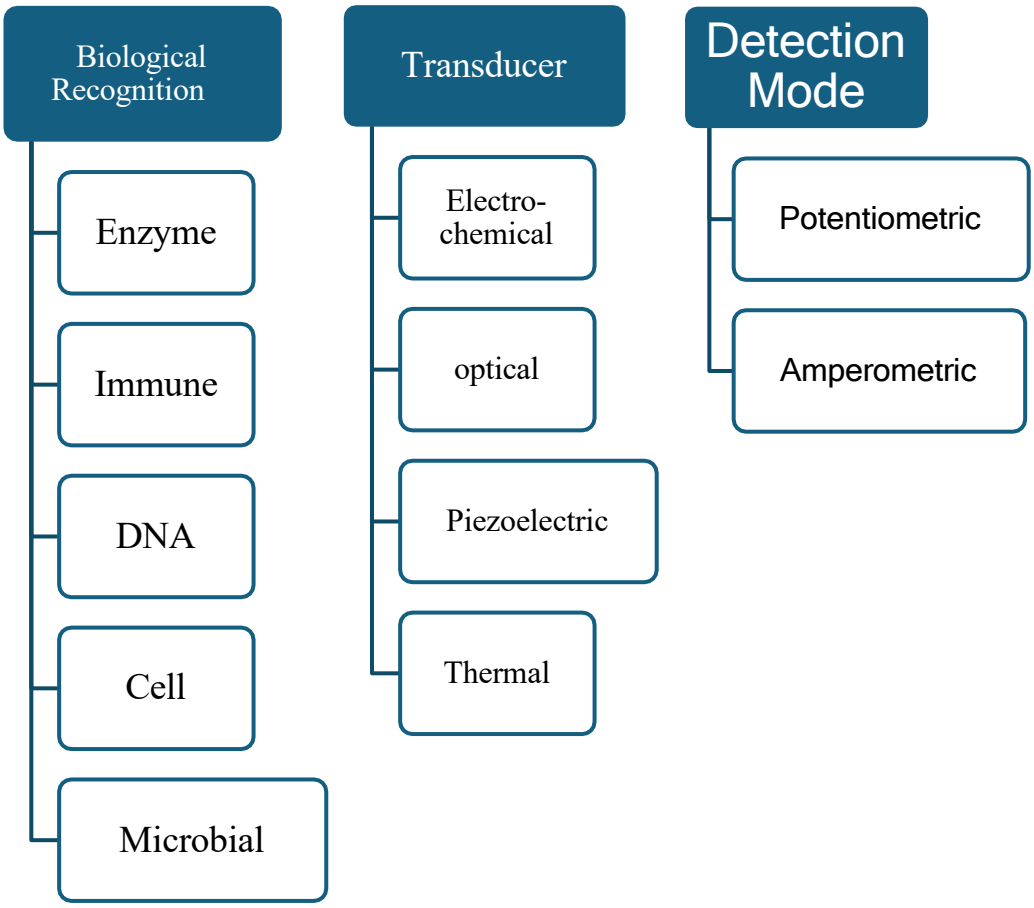

Fig. 1.4 Components of Biosensor

1.5.4.1 Based on the Biological Recognition Element

The biological element interacts with the analyte. Different recognition elements define the specificity and selectivity of the biosensor:

- **Enzymatic Biosensors:**

  Use enzymes as the biological sensing element. The enzyme reacts specifically with the analyte, producing a measurable product. Example: Glucose biosensors using glucose oxidase.

- **Immunosensors:**

  Employ antibodies or antigens to detect specific molecules. They are highly selective and widely used in medical diagnostics, including the detection of pathogens and biomarkers.

- **DNA Biosensors (Genosensors):**

  Use nucleic acids (DNA or RNA) to detect complementary sequences. These are used in genetic testing, disease detection, and forensic analysis.

- **Cell-Based Biosensors:**
  Use whole living cells to detect analytes by measuring cell responses, such as metabolic changes or toxicity.
- **Microbial Biosensors:**
  Utilize microorganisms to detect environmental pollutants or toxins. Changes in microbial activity are converted into measurable signals.

1.5.4.2 Based on the Type of Transducer

The biochemical interaction is translated by the transducer into a detectable output signal. Biosensors can be classified by the physical signal they generate:

- **Electrochemical Biosensors:**
  The sensing mechanism relies on monitoring changes in electrical signals, including current, potential, or impedance, that arise from the biochemical reaction. Examples include amperometric, potentiometric, and conductometric biosensors.
- **Optical Biosensors:**
  Detect changes in light properties, such as absorption, fluorescence, luminescence, or refractive index. Example: Surface plasmon resonance (SPR) sensors are used for detecting biomolecular interactions.
- **Piezoelectric Biosensors:**
  Detect changes in mass or mechanical vibrations on a crystal surface caused by analyte binding. Example: Quartz crystal microbalance (QCM) sensors.
- **Thermal or Calorimetric Biosensors:**
  Measure changes in heat produced or consumed during a biochemical reaction.

1.5.4.3 Based on the Detection Mode or Signal Output

Biosensors can also be classified by how the output is measured and presented:

- **Amperometric Biosensors:**

  Measure the current produced by redox reactions between the analyte and the enzyme.

- **Potentiometric Biosensors:**
  Measure the change in potential (voltage) caused by the biochemical reaction at an electrode.

- **Conductometric Biosensors:**

  Detect changes in the Electrical conduction capability of the medium as the analyte reacts with a

biological element.

- **Optoelectrode-Based Biosensors:**

  Use optical fibres to detect changes in light caused by the biochemical reaction.

1.5.5 Applications of Biosensors

Biosensors are analytical devices that convert biological reactions into measurable signals, making them highly useful across various domains. Their **high specificity, sensitivity, and rapid response** allow them to detect biological, chemical, and environmental changes in real- time [54]. Below is a detailed overview of their major applications:

1. **Medical and Clinical Applications**

   Biosensors have revolutionized healthcare by enabling rapid diagnostics, continuous monitoring, and point-of-care testing. Glucose biosensors that use the enzyme glucose oxidase are widely used by diabetic patients. These devices measure blood sugar levels quickly, accurately, and with minimal sample volume, helping in effective disease management. Biosensors can detect specific proteins, hormones, or enzymes that serve as biomarkers for diseases such as cancer, cardiovascular disorders, liver dysfunction, and infectious diseases [55]. For example, troponin sensors help detect heart attacks early. Portable biosensors allow healthcare professionals to perform rapid tests in clinics, homes, or remote areas without relying on centralized laboratory facilities. Therapeutic drug monitoring is made easier with biosensors that measure drug concentrations in blood, ensuring proper dosing and reducing side effects. Immunosensors and DNA biosensors are used for rapid detection of pathogens such as HIV, influenza virus, and COVID-19, providing early and reliable diagnosis [56].

2. **Environmental Monitoring**

   Biosensors play a critical role in environmental science by detecting pollutants and toxic substances. Biosensors can detect heavy metals (lead, mercury, cadmium), pesticides, nitrates, and microbial contaminants in drinking water, rivers, and wastewater. Microbial biosensors or enzyme-based sensors are commonly used for this purpose. Biosensors help monitor harmful gases such as carbon monoxide, nitrogen oxides, sulfur dioxide, or volatile organic compounds (VOCs). Optical and electrochemical biosensors are often used to detect these airborne pollutants. Soil biosensors detect toxic chemicals, pesticides, and nutrient levels to optimize agricultural practices and prevent environmental contamination. Biosensors can assess the toxicity of environmental samples by monitoring biological responses in microorganisms or cells exposed to pollutants [57].

3. **Food and Agriculture Applications**

In food safety and agriculture, biosensors ensure product quality and monitor for contaminants: they detect harmful bacteria such as Salmonella, E. coli, and Listeria in food and beverages, helping prevent foodborne illnesses [58,59]. Electrochemical and enzymatic biosensors detect residual pesticides on fruits, vegetables, and grains. This helps maintain safety standards and regulatory compliance. Biosensors can measure the sugar, protein, or fat content of food products and assess freshness or spoilage by detecting metabolic by-products, such as ethanol or amines. In agriculture, biosensors measure soil nutrients, pH, and plant stress markers, enabling precision farming and improved crop yield [60].

4. **Industrial and Biotechnological Applications**

Biosensors are essential for industrial process monitoring and quality control. Enzyme and microbial biosensors monitor substrate consumption, metabolite production, and oxygen levels during fermentation across industries such as brewing, dairy, and pharmaceuticals. Biosensors help maintain optimal conditions in bioreactors by continuously monitoring key parameters, improving yield and reducing waste [61]. Biosensors monitor effluents for toxins and pollutants before discharge into the environment, ensuring compliance with environmental regulations. Biosensors monitor the activity of microorganisms that degrade environmental pollutants, providing real-time feedback on remediation efficiency [62].

5. **Forensic and Security Applications**

Biosensors are increasingly used in law enforcement and security due to their rapid, specific detection capabilities: they can identify trace amounts of explosives, chemical warfare agents, or toxic substances at checkpoints or in contaminated areas. DNA biosensors or immunosensors can detect biological evidence, such as blood or tissue markers, helping forensic investigations. Biosensors rapidly detect harmful pathogens or biohazards in public spaces or food/water supplies, providing critical early warning [63].

6. **Research and Development Applications**

In laboratories, biosensors are invaluable tools for studying biological systems: Biosensors monitor molecular interactions in real time, helping identify potential drug candidates and evaluate their effects. DNA or RNA biosensors detect specific genetic sequences, aiding in the study of genetic disorders and mutations, as well as pathogen detection. Biosensors allow continuous monitoring of enzyme activity, substrate consumption, or metabolite production, providing real-

time insights into cellular processes. Optical biosensors, such as surface plasmon resonance (SPR) sensors, are used to study biomolecular interactions that are critical to drug development and molecular biology research [64].

1.6 2D-Based Nanomaterial

Two-dimensional (2D) nanomaterials are a unique category of nanostructures distinguished by their extremely small thickness, typically ranging from a single atomic layer to a few nanometers, while possessing comparatively large lateral dimensions. Their crystal structure consists of strongly bonded atoms within each layer, whereas the individual layers are held together by weak van der Waals interactions, making them suitable for exfoliation into ultrathin sheets. These materials are commonly obtained from layered precursor compounds via mechanical, chemical, or liquid-phase exfoliation, as well as by bottom-up synthesis. Although the ideal form of a 2D nanomaterial is a monolayer, practical synthesis typically yields nanosheets with fewer than 10 atomic layers. Owing to their remarkable electrical, optical, thermal, and mechanical characteristics, 2D nanomaterials have emerged as promising materials for numerous technological applications. Representative examples include graphene, hexagonal boron nitride (hBN), and transition metal dichalcogenides (TMDCs, MX_2), which are extensively utilized in electronic and optoelectronic devices, chemical and biological sensors, catalysts, energy storage systems, photovoltaic cells, lithium-ion batteries, and high-performance composite materials. [65].

1.6.1 Properties of 2D- Nanomaterial

1. **High Surface Area**

   High surface area is a characteristic of all types of 2D nano-materials. Graphene possess one of the highest specific surface areas of 2630 m^2/g [66]. The performance of nanomaterials in various applications is largely influenced by their interfacial and surface properties. Among these, 2D nanomaterials possess an exceptionally large specific surface area, which facilitates efficient loading and controlled release of therapeutic agents. Consequently, they have attracted considerable interest as potential materials for next-generation drug delivery platforms [67]. Ultrathin 2D nanomaterials differ from their bulk counterparts in that they enable control of device performance by providing an atomically thin interface [68].

2. **High Intrinsic Mobility**

   The high charge-carrier mobility of 2D nanomaterials is another fascinating feature that makes them extremely valuable for solar and other applications. 2D nanomaterials, such as black phosphorus, 2D perovskite active layers, TMDs, and highly regarded graphene, have demonstrated

high carrier mobility. Graphene possesses an exceptionally high carrier mobility of 200,000 $cm^2 V^{-1} s^{-1}$. Similarly, the field-effect carrier mobility of electrons in few-layered black phosphorus was measured at about 1000 $cm^2V^{-1}s^{-1}$; for holes, it was about 286 $cm^2V^{-1}s^{-1}$ [69]. The 2D BN was used to develop a nanocomposite paper containing nano-fibrillated cellulose, which exhibited a high thermal conductivity of 145.7 W/m · K. The thermal conductivity of the randomly distributed nanosheets in 2D BN composites was comparable to that of aluminium alloys [70]. In general, two-dimensionality plays a critical role in the transport of fast electrons and ions [71]. The thermal and electrical properties of the desired nanocomposites can be tuned by appropriately doping the 2D nanomaterials [72].

3. Flexibility

The flexibility of 2D nanomaterials is a key, highly desirable characteristic and is extremely useful for designing flexible electronics and sensors. For example, traditional semiconductor- and metal-based strain sensors are fragile and rigid, making them difficult to integrate into wearable electronics. Due to high flexibility, 2D nanomaterials are an excellent choice for developing flexible sensors [73] and other electronic devices [74]. Several 2D nanomaterials have been applied or shown tremendous potential for creating flexible devices, including MXenes, borophenes, and TMDs [75].

4. Intercalation/Host–Guest Relation

Layered 2D nanomaterials are an excellent choice for the intercalation of various species, ranging from ions to atoms and from atoms to molecules. Intercalation is a phenomenon in which the host or foreign species reversibly intercalates into the crystal gaps [76]. The 2D layered MnO_2 has shown impressive intercalation/deintercalation of various metal ions, including K^+, Na^+, Li^+, and Mg^{2+} [77]. Cation diffusion can be controlled by adjusting the interlayer distance. Similarly, MXene has also demonstrated strong intercalation capacity for Na+ and K+ ions for energy storage applications [78]. Thus, this intercalation feature can be extensively exploited in the energy, environmental, catalyst, and medicinal sectors.

5. Semiconductor and Band Gap Tunability

The 2D nanomaterials possess a range of unique properties. As discussed, some properties apply to all 2D nanomaterials, while others are specific to individual families or certain 2D nanomaterials, making them suitable for specific applications. For instance, graphene is a highly rated 2D nanomaterial due to its lack of a band gap; however, its semi-metallic nature limits its use in digital electronics. Several 2D nanomaterials have been reported to exhibit tunable band

gaps and exceptional semiconducting properties [79, 80]. 2D semiconducting nanomaterials with high carrier mobility and a large band gap have received significant attention for digital devices. Most reported 2D nanomaterials exhibit a band gap of 1- 2.4 eV [81]. As the band gap increased, the carrier mobility of the materials decreased . TMD materials have an electronic band gap that increases as the sheet thickness decreases [82]. Bulk TMDs are indirect-band-gap materials that, remarkably, become direct-band-gap materials when reduced to ultrathin sheets. 2D semiconducting nanomaterials are preferred over 3D bulk semiconductors due to their smooth, atomically thin layers, high carrier mobility, and significant stability, whereas 3D bulk semiconductors degrade rapidly during operation [83].

6. Unique Optical Properties

2D nanomaterials exhibit remarkable optical properties, driving intensive research in this field. Unconventional optical properties are observed when ultrathin 2D nanomaterials approach single- or a few-atomic-layer thicknesses. The unique optical properties may include plasmonic effects, light sensitivity, emission, and absorption [84]. Atomic-level ultrathin sheets can be transparent in the visible region. Graphene, the well-known 2D nanomaterial, exhibits excellent optical transparency of 97.7%. The colloidal suspensions of the MXenes are also transparent. The $Ti_3C_2T_z$ thin films demonstrated 97% optical transparency [85], almost equal to that of graphene. The sensitivity of 2D nanomaterials to the external environment and their optical properties have drawn significant interest in the development of optical sensors [86]. Furthermore, the X-ray attenuation and optical properties of 2D nanomaterials can be effective for radiotherapy or phototherapy of cancer [87]. 2D nanomaterials are also being explored for bioimaging [88]. The 2D nanomaterial family is continually expanding, and these properties have not yet been fully explored.

7. High Mechanical Stability

2D nanomaterials exhibit excellent mechanical strength and can withstand stress exceptionally well. 2D nanomaterials have been reported to exhibit high Young's moduli. For most of the 2D nanomaterials, Young's modulus appeared between 150 and 400 GPa [89]. Ti_3C_2 MXene Young's modulus is measured at about 333 ± 30 GPa, one of the highest in solution-processable 2D nanomaterials. It is interesting to note that Young's modulus, theoretically determined using molecular dynamics simulations for Ti_3C_2, is about 502 GPa [90]. The surface termination group may play a critical role in deciding the mechanical stability of the 2D nanomaterials. For instance, the elastic stiffness of the -F and –OH group terminated is lower compared to -O terminated MXenes [91]. Overall, 2D nanomaterials are an excellent choice for enhancing the mechanical

properties of composites as nanofillers and for constructing advanced machines with high mechanical stability [92,93].

1.6.2 Applications

In addition to graphene, a wide range of two-dimensional (2D) nanomaterials has demonstrated remarkable potential in numerous scientific and industrial applications owing to their distinctive electrical, optical, mechanical, and physicochemical properties. Some of the major applications are summarized below:

- **Field-Effect Transistors and Sensors**: Semiconducting 2D materials, including transition metal dichalcogenides (TMDCs) and black phosphorus, have emerged as promising channel materials for field-effect transistors (FETs). Their moderate bandgap and excellent carrier mobility enable efficient charge transport, making them well-suited for high-performance electronic devices and highly sensitive sensing platforms [94].
- **Photodetection**: Owing to their tunable bandgap in the visible and near-infrared spectral regions, along with efficient charge transport characteristics, TMDCs and black phosphorus have been widely explored for photodetector applications. These materials exhibit rapid photo-response and enhanced light absorption, making them attractive for advanced optoelectronic devices. [95].
- **Electrode Material for Energy Storage**: Two-dimensional nanomaterials have gained considerable attention as electrode materials for rechargeable batteries because of their large specific surface area, superior electrical conductivity, and ability to accommodate a high concentration of ions. Although graphene has been extensively employed for this purpose, metallic-phase (1T) molybdenum disulfide (MoS_2) has recently emerged as an effective alternative, offering improved power and energy storage capabilities [96].
- **Topologic Insulators**: Certain 2D materials possess unique electronic structures that enable electrical conduction along their edges while maintaining insulating behavior within the bulk. Materials belonging to the Xene family, as well as tungsten ditelluride (WTe_2), are being actively investigated for topological electronic applications. Notably, WTe_2 can undergo reversible transitions between topological insulating and superconducting states under an applied electric field [97].
- **Valleytronics**: Valleytronics is an emerging branch of semiconductor technology that exploits the valley degree of freedom of charge carriers for information processing. Transition metal dichalcogenides exhibit strong valley polarization, making them promising candidates for next-generation valleytronic devices with potential applications in low-power electronics and quantum technologies [98].
- **Antibacterial Material**: Beyond graphene, several 2D nanomaterials have demonstrated effective

antimicrobial activity. Their ultrathin morphology, high surface reactivity, and favorable biocompatibility contribute to efficient bacterial inactivation, making them suitable for biomedical coatings and antimicrobial surfaces. [99].

- **Drug Delivery**: The exceptionally high surface area and tunable surface chemistry of 2D nanomaterials enable efficient loading of therapeutic agents and controlled drug release. These characteristics have stimulated extensive research into their application as nanocarriers for targeted and sustained drug delivery. [100].
- **Biomedical Engineering**: Two-dimensional nanomaterials are increasingly incorporated into polymeric nanocomposites and hydrogel systems to improve their mechanical strength, stability, and functional performance. Their integration has broadened their use in tissue engineering, regenerative medicine, and other biomedical applications. [101].
- **Biosensing and Gene Sequencing**: Due to their atomic-scale thickness, excellent electrical conductivity, and high sensitivity to surface interactions, 2D nanomaterials have become attractive materials for biosensors and nucleic acid sequencing technologies. Their unique structural characteristics facilitate rapid and accurate detection of biological molecules [102, 103].

References

1. Kavya, S.Kiran, Pesticide chemistry and pharmaceutical chemistry.
2. L.C. Clark, and C. Lyons (1962), Electrode systems for continuous monitoring in cardiovascular surgery, Annals of the New York Academy of Sciences, 102:29–45
3. D. R. Thevenot, K. Toth, R. A. Durst and G. S. Wilson (2001), Electrochemical biosensors: recommended definitions and classification, Biosensors and Bioelectronics, 16:121–131.
4. P. D'Orazio (2011), Biosensors in clinical chemistry, Clinica Chimica Acta, 412:1749–1761
5. O. Lazcka, F.J. Del Campo and F.X. Munoz (2007), Pathogen detection: A perspective of traditional methods and biosensors, Biosensors and Bioelectronics, 22:1205–1217
6. R. Monosik, M. Stred'ansky, and E. Sturdik (2012), Biosensors—classification, characterization and new trends, Acta Chimica Slovaca, 5:109–120
7. C.I.L Justino, A.C. Duarte, and T.A.P. Rocha-Santos (2017), Recent progress in biosensors for environmental monitoring: A review, Sensors, 17:2918.
8. S. Sharma, H. Byrne, and R.J. O'Kennedy (2016), Antibodies and antibody-derived analytical biosensors, Essays in Biochemistry, 60:9–18
9. A.P.F Turner (2013), Biosensors: sense and sensibility, Chemical Society Reviews, 42:3184–3196
10. N.J. Ronkainen, H.B Halsall, and W.R. Heineman (2010), Electrochemical biosensors, Chemical Society Reviews, 39:1747–1763
11. P. Mehrotra (2016), Biosensors and their applications, Journal of Oral Biology and Craniofacial Research, 6:153–159
12. B.R. Eggins (2002), Chemical Sensors and Biosensors, Wiley.
13. J. Wang (2006), Analytical Electrochemistry (3rd ed.), Wiley.
14. A. Sassolas, L.J. Blum, and B.D. Leca-Bouvier (2012), Immobilization strategies to develop enzymatic biosensors, Biotechnology Advances, 30:489–511
15. M.N. Velasco-Garcia (2009), Biosensors for environmental monitoring, Biosensors and Bioelectronics, 24:849–859
16. D. Grieshaber et al. (2008), Electrochemical biosensors: sensor principles and architectures, Sensors, 8:1400–1458
17. M. Song et al. (2021), Materials and methods of biosensor interfaces with stability, Frontiers in Materials, 8:705661.

18. O. Smutok, and E. Katz (2023), Biosensors: Electrochemical devices—General concepts and performance, Biosensors, 13:44

19. V. Naresh, and N. Lee (2021), A review on biosensors and recent development of nanostructured materials-enabled biosensors, Sensors, 21:1109

20. C.S. Pundir, and V. Narwal (2018), Biosensors and their applications, Applied Biochemistry and Biotechnology, 186:679–701.

21. M. Ramesh et al. (2023), Nanotechnology-enabled biosensors: fundamentals and design principles, Biosensors, 13:40

22. S. Malik et al. (2023), Nanomaterials-based biosensors and their applications, Heliyon, 9:e19929

23. P. Singh et al. (2016), Biomedical perspective of electrochemical nanobiosensor, Nano-Micro Letters, 8:193–203

24. A. Banerjee et al. (2021), Nanotechnology for biosensors: A review, Materials Advances, 2:4890–4921.

25. A. P. F. Turner (2013), "Biosensors: sense and sensibility," Chemical Society Reviews, 42:3184-3196.

26. S. M. Borisov and O. S. Wolfbeis (2008), Optical biosensors, Chemical reviews, 108:423-461.

27. M. Pohanka (2017), The piezoelectric biosensors: principles and applications, A review, International Journal of Electrochemical Science, 12:496-506.

28. K. Ramanathan and B. Danielsson (2001), Principles and applications of thermal biosensors, Biosensors and Bioelectronics, 16:417-423.

29. P. Tetyana, P. M. Shumbula, and Z. Njengele-Tetyana (2021), Biosensors: Design, development and applications, In Nanopores, IntechOpen.

30. E. Karami and F. Kazemi-Lomedasht (2022), Biosensors: Types, features, and application in biomedicine, Asian Pacific Journal of Tropical Biomedicine, 12:367-373

31. A. R. Ndhlala, A. K. Yuksel, N. Celebi, and H. O. Dogan (2023), A General Review of Methodologies Used in the Determination of Cholesterol Levels in Foods, Foods, 12:4424.

32. A. Haleem, M. Javaid, R. P. Singh, R. Suman, and S. Rab (2021), Biosensors applications in medical field: A brief review, Sensors International, 2:100100.

33. M. Srivastava, N. Srivastava, P. K. Mishra, and B. D. Malhotra (2021), Prospects of nanomaterials-enabled biosensors for COVID-19 detection, Science of The Total Environment, 754:142363.

34. C. Karunakaran, R. Rajkumar, and K. Bhargava (2015), Introduction to Biosensors,

Biosensors and Bioelectronics, Elsevier, 1-68.

35. S. Bobade, D. R. Kalorey, and S. Warke (2016), Biosensor Devices: A review on their biological applications, Bioscience Biotechnology Research Communications, 9:132-137.

36. S. K. Arya, A. Chaubey, and B. D. Malhotra (2006), Fundamentals and applications of biosensors, Proceedings-Indian National Science Academy, 72:249.

37. J. D. Munzar, A. Ng. and D. Juncker (2019), Duplexed aptamers: History, design, theory, and application to biosensing, Chemical Society Reviews, 48:1390-1419.

38. J. P. Chambers, B. P. Arulanandam, L. L. Matta, A. Weis, and J. J. Valdes (2008), Biosensor recognition elements, Current issues in molecular biology, 10:1-12.

39. A. P. F. Turner (2013), Biosensors: Sense and sensibility, Chemical Society Reviews, 42:3184–3196

40. J. Kaur, S. Choudhary, R. Chaudhari, R. D. Jayant, and A. Joshi (2019), Enzyme-based biosensors, Bioelectronics and Medical Devices, 211-240.

41. L. Alvarado-Ramirez, M. Rostro-Alanis, J. Rodriguez-Rodriguez, J. E. Sosa-Hernández, E. M. Melchor-Martinez, H. M. N. Iqbal, and R. Parra-Saldivar (2021), Enzyme (single and multiple) and nanozyme biosensors: Recent developments and their novel applications in the water-food-health nexus, Biosensors, 11:410.

42. M. Polanka (2015), Biosensors containing acetylcholinesterase and butyrylcholinesterase as recognition tools for detection of various compounds, Chemical Papers, 69:4-16

43. M. Aizawa (1994), Immunosensors for clinical analysis, Advances in clinical chemistry, 31:247-275.

44. S.J. Updike, and G.P. Hicks (1967), The enzyme electrode, Nature, 214:986–988

45. D. Grieshaber et al. (2008), Electrochemical biosensors—Sensor principles and architectures, Sensors, 8:1400–1458

46. J. Fraden (2010), Handbook of Modern Sensors: Physics, Designs, and Applications (4th ed.), Springer

47. V. Naresh, and N. Lee (2021), A review on nanostructured material-enabled biosensors, Sensors, 21:1109

48. A.J. Bard, and L.R. Faulkner (2001), Electrochemical Methods: Fundamentals and Applications (2nd ed.), Wiley.

49. Y. Du and S. Dong (2017), Nucleic acid biosensors recent advances and perspectives, Analytical chemistry, 89:189-215

50. K. Länge, F. Bender, A. Voigt, H. Gao, and M. Rapp (2003), A surface acoustic wave biosensor concept with low flow cell volumes for label-free detection, Analytical

chemistry, 75:5561-5566.

51. R. Ahmad and M. Sardar (2015), Enzyme immobilization: an overview on nanoparticles as immobilization matrix, Biochemistry and Analytical Biochemistry, 4:1000178

52. M. Asal, O. Ozen, M. Sahinler, H. T. Baysal, and 1. Polatoglu (2019), An overview of biomolecules, immobilization methods and support materials of biosensors, Sensor Review, 39:377-386.

53. T. Bhardwaj (2014), A review on immobilization techniques of biosensors, International Journal of Engineering Research & Technology, 3:294-298

54. A. Sassolas, L. J. Blum, and B. D. Leca-Bouvier (2012), Immobilization strategies to develop enzymatic biosensors, Biotechnology Advances, 30:489-511

55. A. Amine and H. Mohammadi (2018), Amperometry, In reference Module in Chemistry, Molecular Sciences and Chemical Engineering, 10:204

56. B. J. Birch and T. E. Edmonds (1988), Potentiometric transducers, Chemical Sensors, Springer, 1:214-224

57. A. Brecht and G. Gauglitz (1997), Recent developments in optical transducers for chemical or biochemical applications, Sensors and Actuators B: Chemical, 38:1-7

58. G. Liu, and Y. Lin (2007), Electrochemical immunosensors, Talanta, 74:308–317

59. T.G. Drummond, M.G. Hill, and J.K. Barton (2003), Electrochemical DNA sensors, Nature Biotechnology, 21:1192–1199

60. J.J. Pancrazio et al. (2017), Living cell-based biosensors, Annual Review of Biomedical Engineering, 19:455–476

61. N. Verma, and M. Singh (2005), Biosensors for environmental monitoring: A review, Applied Biochemistry and Biotechnology, 128:121–139

62. Y. Lei, W. Chen, and A. Mulchandani (2006), Microbial biosensors, Applied Microbiology and Biotechnology, 72:1135–1144

63. P. Banerjee, and A.K. Bhunia (2010), Cell-based biosensors for pathogens, Biosensors and Bioelectronics, 26:99–106

64. A. Sassolas, L.J. Blum, and B.D. Leca-Bouvier (2008), DNA biosensors and microarrays, Chemical Reviews, 108:109–139

65. Z. Rafiei-Sarmazdeh, S.M. Zahedi-Dizaji, and A. Kafi Kang (2019), Two-Dimensional Nanomaterials. In S. Ameen (Ed.), Nanostructures, IntechOpen.

66. J. Zeng, X. Ji, Y. Ma, Z. Zhang, S. Wang, and Z. Ren, et al. (2018) 3D graphene fibers grown by thermal chemical vapor deposition, Advanced Materials, 30:1705380

67. M. Qiu, W.X. Ren, T. Jeong, M. Won, G.Y. Park, and D.K. Sang, et al. (2018),

Omnipotent phosphorene: A next-generation, two-dimensional nanoplatform for multidisciplinary biomedical applications, Chemical Society Reviews, 47:5588-5601

68. Z. Hu, Z. Wu, C. Han, J. He, Z. Ni, and W. Chen (2018), Two-dimensional transition metal dichalcogenides: Interface and defect engineering ,Chemical Society Reviews, 47:3100-3128

69. J. Xiao, M. Long, X. Zhang, J. Ouyang, H. Xu, and Y. Gao (2015), Theoretical predictions on the electronic structure and charge carrier mobility in 2D Phosphorus sheets, Scientific Reports, 5:9961.

70. H. Zhu, Y. Li, Z. Fang, J. Xu, F. Cao, and J. Wan, et al. (2014), Highly thermally conductive papers with percolative layered boron nitride nanosheets, ACS Nano, 8:3606-3613

71. Q. Guo, N. Chen, and L. Qu (2020), Two-dimensional materials of group-IVA boosting the development of energy storage and conversion, Carbon Energy, 2: 54- 71

72. J. Joy, E. George, P. Haritha, S. Thomas, and S. Anas (2020), An overview of boron nitride based polymer nanocomposites, Journal of Polymer Science, 58:3115- 3141

73. Q. Zheng, J. Lee, X. Shen, X. Chen, and J.-K. Kim (2020), Graphene-based wearable piezoresistive physical sensors, Matterials Today, 36:158- 179

74. X. Peng, L. Peng, C. Wu, and Y. Xie (2014), Two dimensional nanomaterials for flexible supercapacitors, Chemical Society Reviews, 43: 3303-3323

75. Y. Li, R. Wang, Z. Guo, Z. Xiao, H. Wang, and X. Luo (2019), Emerging two-dimensional noncarbon nanomaterials for flexible lithium-ion batteries: Opportunities and challenges; Journal of Materials Chemistry A, 7:25227-25246

76. Y. Jung, Y. Zhou, and J.J. Cha (2016), Intercalation in two-dimensional transition metal chalcogenides, Inorganic Chemistry Frontiers, 3:452-463

77. P. Xiong, R. Ma, N. Sakai, X. Bai, S. Li, and T. Sasaki (2017), Redox Active Cation Intercalation/Deintercalation in Two-Dimensional Layered MnO2 Nanostructures for High-Rate Electrochemical Energy Storage, ACS Applied Materials and Interfaces, 9:6282-6291.

78. M.K. Aslam, and M. Xu (2020), A Mini-Review: MXene composites for sodium/potassium-ion batteries, Nanoscale, 1 2 : 15993-16007

79. F. Zhao, Y. Feng, Y. Wang, X. Zhang, X. Liang, and Z. Li et al. (2020), Two-dimensional gersiloxenes with tunable bandgap for photocatalytic H_2 evolution and CO_2 photoreduction to CO. Nature Communications, 11:1–13.

80. Y. Wang, L. Wang, X. Zhang, X. Liang, Y. Feng, and W. Feng (2021), Two-dimensional

nanomaterials with engineered bandgap: Synthesis, properties, applications, Nano Today, 37:101059

81. S. Kang, D. Lee, J. Kim, A. Capasso, H.S. Kang, and J.-W. Park, et al. (2020), 2D semiconducting materials for electronic and optoelectronic applications: Potential and challenge, 2D Materials 7:022003

82. F. Schwierz, J. Pezoldt, and R. Granzner (2015), Two-dimensional materials and their prospects in transistor electronics, Nanoscale, 7:8261-8283

83. Q.H. Wang, K. Kalantar-Zadeh, A. Kis, J.N. Coleman, and M.S. Strano (2012), Electronics and optoelectronics of two-dimensional transition metal dichalcogenides, Nature Nanotechnology, 7:699-712

84. S.K. Su, C.P. Chuu, M.Y. Li, C.C. Cheng, H.S.P. Wong, and L.J. Li (2021), Layered Semiconducting 2D Materials for Future Transistor Applications, Small Structures, 2:2000103.

85. Y. Zheng, F.Z. Sun, X. Han, J. Xu, and X.H. Bu (2020), Recent Progress in 2D Metal-Organic Frameworks for Optical Applications, Advanced Optical Materials, 8:2000110

86. A.D. Dillon, M.J. Ghidiu, A.L. Krick, J. Griggs, S.J. May, and Y. Gogotsi, et al. (2016), Highly Conductive Optical Quality Solution-Processed Films of 2D Titanium Carbide, Advanced Functional Materials, 26:4162-4168

87. M. Devi (2020), Application of 2D Nanomaterials as Fluorescent Biosensors, In Fluorescent Nanomaterials for Sensing and Imaging, ACS Symposium Series, 1353:117-141

88. L. Cheng, X. Wang, F. Gong, T. Liu, and Z. Liu (2020), 2D Nanomaterials for Cancer Theranostic Applications, Advanced Materials, 32:1902333

89. K. Khan, A.K. Tareen, M. Aslam, R. Wang, Y. Zhang, and A. Mahmood, et al. (2020), Recent developments in emerging two-dimensional materials and their applications, Journal of Materials Chemistry C, 8:387-440

90. H. Jiang, L. Zheng, Z. Liu, X. Wang (2020), Two-dimensional materials: From mechanical properties to flexible mechanical sensors, InfoMat, 2: 1077-1094

91. M. Carey, M.W. Barsoum (2021), MXene polymer nanocomposites: A review, Materials Today Advances, 9:100120

92. X. Zhan, C. Si, J. Zhou, Z. Sun (2020), MXene and MXene-based composites: Synthesis, properties and environment-related applications, Nanoscale Horizons, 5:235-258

93. M. Park, N. Kim, J. Lee, M. Gu, B.S. Kim (2021), Versatile graphene oxide nanosheets

via covalent functionalization and their applications, Materials Chemistry Frontiers, 5:4424-4444

94. W. Cui, Z.Y. Hu, R.R. Unocic, G. van Tendeloo, X. Sang (2021), Atomic defects, functional groups and properties in MXenes, Chinese Chemical Letters, 32:339-344

95. R. Bayan and N. Karak (2020), Polymer nanocomposites based on two-dimensional nanomaterials, Two-Dimensional Nanostructures for Biomedical Technology: A Bridge between Material Science and Bioengineering, 249-279.

96. M. Dong, H. Zhang, L. Tzounis, G. Santagiuliana, E. Bilotti, and D. G. Papageorgiou (2021), Multifunctional epoxy nanocomposites reinforced by two-dimensional materials: A review, Carbon, 185:57-81.

97. B. Le, J. Khaliq, D. Huo, X. Teng, and I. Shyha (2020), A review on nanocomposites, Part 1: Mechanical properties, Journal of Manufacturing Science and Engineering, 142:100801.

98. J. Zhu, F. M. Uhl, A. B. Morgan, and C. A. Wilkie (2001), Studies on the mechanism by which the formation of nanocomposites enhances thermal stability, Chemistry of Materials, 13:4649-4654.

99. B. Scrosati (1988), Electrochemical properties of conducting polymers, Progress in Solid State Chemistry, 18:1-77.

100. P. Kumbhakar, S. S. Ray, and A. L. Stepanov (2014), Optical properties of nanoparticles and nanocomposites, Journal of Nanomaterials, 1-2

101. T. K. Das and S. Prusty (2012), Review on conducting polymers and their applications, Polymer -Plastics Technology and Engineering, 51:1487-1500.

102. H.M.C. De Azeredo (2009), Nanocomposites for food packaging applications, Food Research International, 42:1240-1253.

103. S. Bera, M. Singh, R. Thantirige, S. K. Tiwary, B. T. Shook, E Nieves, D. Raghavan, A Karim, and N. R. Pradhan (2023), 2D-nanofiller-based polymer nanocomposites for capacitive energy storage applications, Small Science, 3:2300016.

Chapter – 2

Literature Review

2.1 Overview of Organophosphate Pesticides

Organophosphate (OP) pesticides are synthetic chemicals widely used in agriculture to control pests on crops such as fruits and vegetables, as well as in public health efforts, such as mosquito control [1]. Organophosphate (OP) pesticides, introduced in the mid-20th century as less persistent substitutes for organochlorines like DDT, are synthetic phosphorus-based insecticides that dominate global agriculture and public health pest control. They function by phosphorylating acetylcholinesterase (AChE), thereby disrupting acetylcholine hydrolysis in the insect nervous system, triggering overstimulation, paralysis, and death [2,3]. Chemically, OPs feature a central phosphoryl (P=O) group bonded to thiols, alcohols, or alkyl groups, influencing their solubility, stability, and toxicity; prominent examples include chlorpyrifos, malathion, parathion, and diazinon, applied extensively on crops like grains, fruits, vegetables, and cotton, as well as for mosquito eradication in malaria-endemic regions [4]. While effective for boosting yields and vector control, their use raises serious health concerns: acute exposure via skin, inhalation, or ingestion provokes cholinergic crises with SLUDGE symptoms (salivation, lacrimation, urination, defecation, gastrointestinal upset, emesis), while chronic low-dose contact correlates with neurodevelopmental impairments and endocrine interference in humans [5, 6, 7].

Organophosphate pesticides possess this characteristic structure:

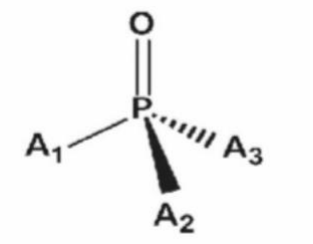

Fig. 2.1 Chemical Structure of an Organophosphate Compound

Environmentally, OPs leach into soil, groundwater, and waterways via runoff, bioaccumulate in non-target organisms such as bees, birds, and fish, and contribute to biodiversity loss despite relatively rapid hydrolysis or microbial breakdown [8,9]. Therefore, this underscores the urgent

need for rapid, accurate, and dependable detection of trace OP levels to safeguard public health and safety, with active research continuing in this field [10].

Organophosphate (OP) pesticides in humans provoke four distinct neurotoxic syndromes via cholinesterase inhibition, oxidative damage, and disruption of neuropathy target esterase (NTE), each with unique timelines, symptoms, and pathological bases [11].

Acute Cholinergic Syndrome

This provides an immediate response, with onset within minutes to hours of substantial exposure, such as dermal, inhalation, or ingestion. Stems from acetylcholinesterase (AChE) phosphorylation, causing acetylcholine overload at muscarinic and nicotinic synapses. Muscarinic effects include miosis, hypersalivation, sweating, bronchorrhea, bradycardia, hypotension, nausea, vomiting, diarrhoea, and urinary incontinence (such as diarrhoea, urination, bronchorrhea, emesis, lacrimation, salivation). Nicotinic signs feature muscle fasciculations, tremors, weakness, tachycardia, hypertension, and paralysis; central effects add confusion, seizures, coma, and respiratory arrest from diaphragmatic failure, with mortality up to 10-20% untreated [12,13,14, 15].

Intermediate Syndrome (IMS)

Intermediate Syndrome (IMS) emerges 1-4 days post-acute phase resolution (typically 24-96 h). IMS affects (~40-60%) of severe cases, independent of cholinergic signs, due to prolonged AChE inhibition at neuromuscular junctions, causing postsynaptic dysfunction and muscle necrosis [16,17]. Key features include neck muscle weakness and respiratory failure from intercostal or diaphragm paralysis, often requiring ventilation for 4-21 days and recovery spans weeks with physiotherapy [18]. IMS mainly strikes people who had a severe initial poisoning from heavy AChE blockage, causing ongoing high acetylcholine levels at muscle- nerve connections, but it doesn't hit everyone who gets exposed [19].

Organophosphate Induced Delayed Polyneuropathy (OPIDP)

This nerve damage starts 5 days to 3 weeks after exposure (worst around 2-3 weeks), caused by over 70% blockage of NTE enzyme plus "aging" (chemical breakdown), which triggers axon breakdown from messed-up calcium levels and protein shredding in spinal cord motor cells and peripheral nerves [20,14]. Signs start with tingling in hands/feet, burning foot pain, leg cramps, then weak or floppy leg paralysis, loss of reflexes, unsteadiness, foot drop, and arm issues, it lingers 3-12 months with partial recovery, hitting men more and linked to fat- soluble OPs like tri-orthocresyl phosphate [21]. Signs of OPIDP include upper motor neuron signals, a high-stepping

walk with both feet dragging, and in worst cases, full-body paralysis with dropped feet and wrists [11,22]. While peripheral nerve recovery can improve significantly over time, severe cases may leave lasting spastic unsteadiness due to the degree of upper motor neuron damage [23].

Chronic Organophosphate-Induced Neuropsychiatric Disorder (COPIND)

COPIND shows up weeks or months after a serious poisoning episode or from ongoing low- dose contact, stemming from lasting brain dysfunction due to excess cholinergic activity, low dopamine levels, leaky blood-brain barrier, and brain swelling [24]. Key signs are ongoing worry, sadness, mental breakdowns, mood swings, forgetfulness, confusion, seeing things, sleep issues, and mild thinking problems spotted through brain tests; it's tied to cell damage from stress, enzyme overdrive, and messed-up growth signals, often lasting variably with limited fix [25,26].

Detecting organophosphate (OP) pesticides is essential because of their widespread agricultural use, which often contaminates food, water, soil, and air, posing risks to human health, including acute poisoning and chronic neurotoxicity [27].

Detecting OP Pesticides: Farmers spray organophosphate (OP) pesticides widely on fruits, veggies, grains, and cotton to kill bugs, but leftovers spread into food, drinking water, rivers, soil, and even air through spray drift or runoff, risking serious harm to humans like instant poisoning, nerve damage, kids' brain growth issues, cancer links, and deaths—plus wiping out bees, fish, birds, and other wildlife via food chain buildup [28, 29].

Health Protection: Catching tiny traces (like parts per billion) helps to stop food poisoning outbreaks and allows doctors to treat exposed areas early with antidotes like atropine to protect guards, farm workers, and kids from daily low doses, which causing delay learning or Parkinson 's-like symptoms and also helps to track residues in blood or urine for lawsuits or bans [30,31,32].

Environmental Safeguard: Monitors farm runoff polluting lakes and oceans, killing aquatic life and depleting oxygen, creating "dead zones"; checks for thinning bird eggshells or bee colony crashes; measures soil buildup harming earthworms or crops long-term; and helps restore habitats by spotting hotspots for cleanup [31,1].

Export Importance: Meets strict global rules (EPA, EU MRLs, WHO guidelines) to avoid export rejections costing billions, guides safer farming switches to biopesticides, enables real-time alerts in suicide epidemics or accidents common in Asia or Africa, fuels research for nanosensors or AI detectors, ultimately saves lives, cuts healthcare costs, and protects biodiversity [32,30].

2.2 Literature Review

Nanomaterials have become powerful tools for biological sensing due to their size-dependent physicochemical properties and their ability to be surface-modified for specific functions. The efficient interaction between target biomolecules and nanomaterials is largely attributed to the small size of nanostructures, typically 1-100 nm, which enables selective binding. These features facilitate enhanced adsorption and recognition of biomolecules such as proteins, DNA, and small metabolites [33]. A wide spectrum of nanomaterials, including metallic nanoparticles (such as gold and silver), carbon- based structures (such as graphene and carbon nanotubes), magnetic nanoparticles (Fe_3O_4), and semiconductor quantum dots, has been extensively explored for biosensor development. Therefore, the analytical performance of the developed electrode was evaluated against that reported in earlier studies [34,35]

Table 2.1 Recent developments in the analytical efficiency of electrochemical biosensors for trichlorfon detection

S.No.	Fabricated Electrode	Detection Method	Linear Range	LODs	Ref.
1.	AChE/g-C_3N_4@MoS_2	DPV	5–100 nM	2.1 nM	**[36]**
2.	AChE/Ag@CuO/ITO	DPV	5- 35 nM	1.59 nM	**[37]**
3.	AgNPs–MWCNT modified electrode	Electrochemiluminescence (ECL)	5.0×10^{-8}– 5.0×10^{-11} mol L^{-1}	3.9×10^{-12} mol L^{-1}	**[38]**
4.	MIP/sol–gel/GCE	DPV	10^{-8} – 10^{-6} g mL^{-1}	2.8×10^{-9} g mL^{-1}	**[39]**
5.	Carbon dot (CD)-based nanozyme hydrogel	Colorimetric	0.2- 50 nM	0.16 nM	**[40]**
6.	CuS/MnS/MWCNTs	DPV	1.0–10 and 10–100 nM	0.37 nM	**[41]**
7.	Fe_3O_4@MWNT-COOH/CS	DPV	1.0×10^{-5} to to 1.0×10^{-11} M	8.94×10^{-12} M	**[42]**

2.3 Characteristics of the Material

Developing innovative materials is essential for fabricating high-performance biosensors. Nanostructures with large surface areas, high electrical conductivity, and good biocompatibility are considered highly suitable for biosensor fabrication [43]. Attaching enzymes to these nanostructures enhances biosensor sensitivity, durability, and operational efficiency. Consequently, diverse nanostructures have been integrated onto electrodes to develop enzymatic biosensors, offering an innovative approach to amplify biosensor signals [10]. Among them, two-dimensional (2D) layered nanostructures have significant potential to improve biosensors thanks to their outstanding physicochemical properties, including excellent biocompatibility, large specific surface areas, and optimal charge-transport properties. GCN (g-C_3N_4) aligns well here, as its layered 2D structure supports enzyme loading and provides nitrogen-rich sites that improve electron mediation in the detection of organophosphate pesticides [44].

2.3.1 Graphitic Carbon Nitride (g-C_3N_4)

Graphitic carbon nitride (g-C_3N_4) is a robust, metal-free 2D semiconductor that finds broad utility owing to its 2.7 eV bandgap for visible-light harvesting, exceptional thermal endurance beyond 600°C, and nitrogen-abundant layers that foster catalytic sites [45].

In photocatalysis, it excels at breaking down contaminants like rhodamine B or tetracycline through superoxide and hydroxyl radical pathways, often reaching full mineralization within 90 min under ambient sunlight, while P- or S-doped variants accelerate H_2 generation from water splitting at rates exceeding 4000 μmol h^{-1} g^{-1} with minimal overpotentials [46]. Energy applications leverage g-C_3N_4's pseudocapacitive properties, as in g-C_3N_4/MnO_2 or Co_3O_4 composites [47]. For biosensors, ultra-thin g-C_3N_4 nanosheets promote enzyme conjugation via π-π or electrostatic forces, yielding platforms for acetylcholinesterase-based OPP sensing (LOD 0.005 μM in tap water) or glucose oxidase assays spanning 0.1-20 mM with 48 μA mM^{-1} cm^{-2} sensitivity and 25 reuses at 85% efficiency. Biomedically, its low cytotoxicity (<5% cell death at 200 μg mL^{-1}) supports fluorescence bioimaging (emission ~550nm) and targeted delivery of doxorubicin, where protonation enhances cellular uptake by 3-fold; disulfide grafting further imparts biodegradability for scaffolds in wound healing [48,49]. Environmentally, it selectively adsorbs and detects Hg^{2+} or Cr(VI) down to 0.5 ppb amid interferents, alongside non-enzymatic H_2O_2 reduction at nanozyme rates rivalling those of HRP. These multifaceted roles underscore g-C_3N_4's promise in sustainable technologies. Graphitic carbon nitride (g-C_3N_4 or GCN) powers multiple high-impact applications

through its layered structure, visible-light response, and nitrogen-rich sites [50].

For cleaning water, GCN breaks down dyes like rhodamine B by over 90% in just 80 min, removes antibiotics such as tetracycline in under an hour, and handles chemicals like phenols. Adding small tweaks, such as phosphorus or sulfur doping, can make it 4-6 times faster by helping electrons move more efficiently and reducing wasted energy [51].

In making clean fuels, GCN splits water to produce hydrogen gas at high rates—over 4500 μmol per h per gram—especially when paired with catalysts such as platinum or MoS_2. It also converts CO_2 into useful products such as methanol or carbon monoxide, using its nitrogen sites to bind and convert CO_2 [52,53].

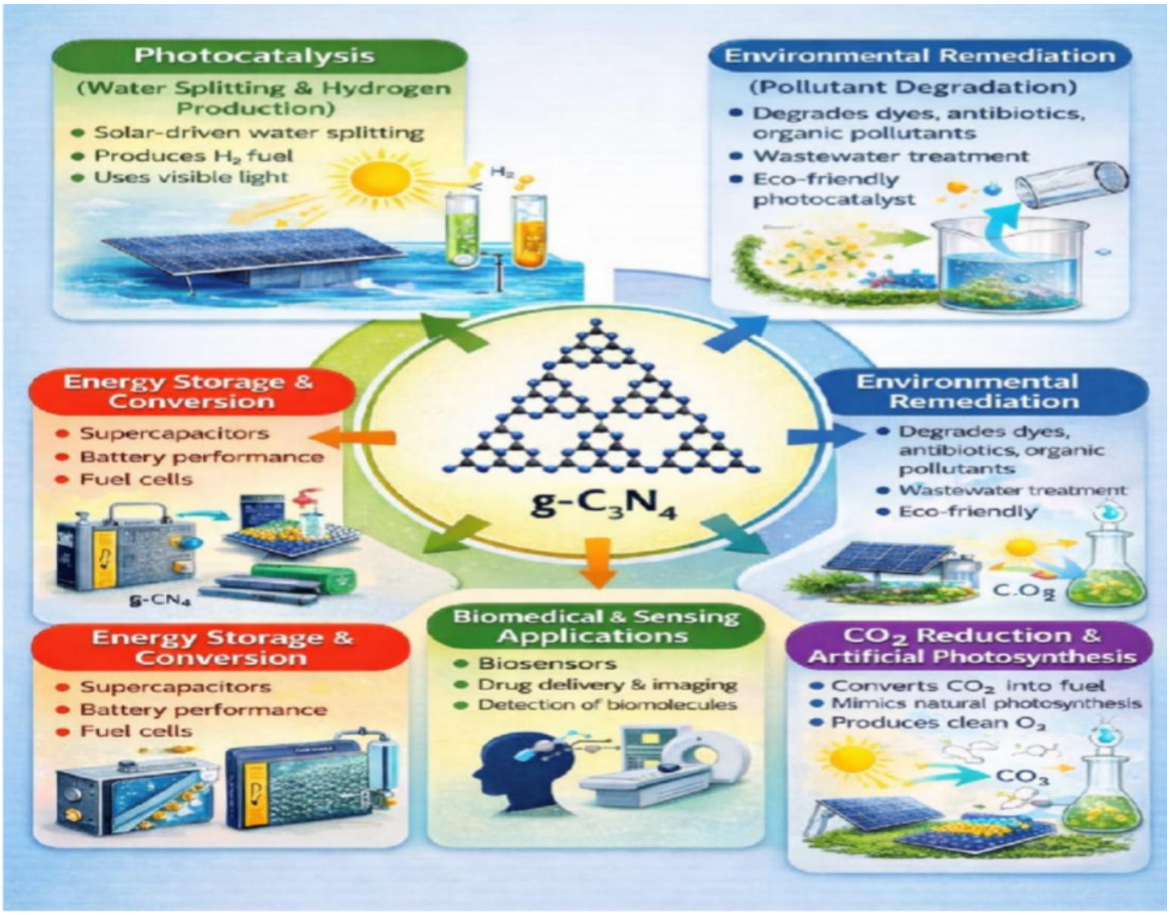

Fig. 2.1 Illustration of Applications of g-C_3N_4

2.3.2 Applications of g-C_3N_4

1. **Biosensor**

Graphitic carbon nitride (g-C_3N_4) has gained significant attention as a transducer material for biosensors because of its semiconductor behaviour, biocompatibility, and rich surface chemistry. In g-C_3N_4-based biosensors, the material acts as a scaffold that immobilizes biological recognition elements (enzymes, antibodies, DNA, aptamers, etc.) while simultaneously serving as an electroactive or photoactive interface that converts the biochemical binding event into a measurable electrical or optical signal [54,55].

The heptazine-based layered structure of g-C_3N_4 provides a planar, π-rich surface that allows strong non-covalent interactions with biomolecules and metal nanoparticles, which can be exploited to design label-free or nanoparticle-enhanced biosensors [56].

These design strategies allow g-C_3N_4-based biosensors to achieve high sensitivity, low detection limits, good selectivity, and stability in complex matrices such as blood, urine, or environmental water samples [57].

2. **Photocatalysis**

In photocatalytic applications, g-C_3N_4 absorbs visible light and generates electron–hole pairs; its moderately negative conduction band and positive valence band enable redox reactions for water splitting, CO_2 reduction, and the degradation of organic pollutants [58]. Photogenerated electrons reduce H^+ to H_2 or O_2 to reactive oxygen species, while holes oxidize water or organic contaminants, but efficiency is limited by charge-carrier recombination, which is mitigated by nano structuring, doping (e.g., S, P), or coupling with oxides such as TiO_2 or ZnO [59].

3. **Energy Storage**

For energy-storage devices such as Li-ion, Li–S, Na-ion, and K-ion batteries as well as supercapacitors, g-C_3N_4 acts as an organic host or separator that chemically stabilizes active species and improves ion diffusion. Its layered framework and nitrogen-rich sites enhance surface redox activity, facilitate charge transfer, and buffer volume changes in anodes, thereby improving capacity retention and rate capability, especially when combined with graphene or other carbon materials [60].

4. Biomedicine

In biomedicine, g-C_3N_4 nanosheets serve as biocompatible platforms for photodynamic therapy, bioimaging, and drug delivery. Under visible light, they generate reactive oxygen species that can selectively kill cancer cells, while their intrinsic fluorescence and tunable surface enable labelling and in vitro/in vivo imaging. Functionalization with targeting ligands or polymers further improves tumor-specific delivery and reduces off-target toxicity [61].

5. Environmental Sensing

For environmental sensing, g-C_3N_4 provides a sensitive transducer for detecting gases (e.g., SO_2, SO_3), heavy metals, and organic pollutants owing to its high surface area and favorable adsorption–electron-transfer properties [62]. In chemiresistive or electrochemical sensors, analyte adsorption alters the charge-carrier density or interfacial resistance of g-C_3N_4, producing a measurable change in current, impedance, or photocurrent that can be correlated to concentration [63, 64].

2.3.3 Ce-NiO

Ce-doped NiO (cerium-doped nickel oxide) nanoparticles are an important class of p-type semiconductor nanomaterials that have attracted considerable attention due to their tunable structural, optical, and electrochemical properties. Nickel oxide (NiO) itself possesses a stable rock-salt cubic structure and is widely used in catalysis, sensing, and energy-related applications; however, its relatively wide band gap and limited electrical conductivity restrict its performance [65,66]. To overcome these limitations, doping with rare-earth ions such as cerium (Ce^{3+}/Ce^{4+}) has been extensively explored. When Ce ions are incorporated into the NiO lattice, they partially substitute Ni^{2+} sites, leading to lattice distortion because of the larger ionic radius of Ce compared to Ni. This substitution generates structural defects such as oxygen vacancies and nickel vacancies, which play a crucial role in modifying the physicochemical behavior of the material [67].

At the nanoscale, Ce doping strongly influences the morphology and growth behavior of NiO nanoparticles [68]. During synthesis processes such as sol–gel, hydrothermal, or co-precipitation methods, Ce ions act as growth inhibitors, reducing particle agglomeration and leading to smaller, more uniform nanoparticles with enhanced surface roughness and porosity. This increase in surface area provides more active sites, which is particularly beneficial for surface-dependent processes such as catalysis and electrochemical sensing [69,70]. From an electronic perspective, Ce doping introduces localized energy states within the band structure of NiO, which leads to a reduction in the optical band gap compared to pure NiO. This band gap narrowing is associated with defect levels created by oxygen vacancies as well as hybridization between Ni 3d and Ce 4f orbitals. As

a result, Ce-doped NiO exhibits improved visible-light absorption and enhanced charge carrier mobility [71].

In electrochemical biosensors, the material enhances electron-transfer kinetics at the electrode–electrolyte interface, resulting in higher sensitivity and lower detection limits [72]. The synergistic interaction between the Ni^{2+}/Ni^{3+} and Ce^{3+}/Ce^{4+} redox couples facilitate rapid charge mediation, while oxygen vacancies facilitate strong adsorption of target analytes, such as pesticides, heavy metal ions, and biomolecules [73]. The superior performance of Ce-doped NiO nanoparticles arises from a combination of structural distortion, defect engineering, band-gap modulation, and dual redox activity, making them highly promising for advanced environmental sensing, biosensing, and catalytic applications [74,75].

2.3.4 Applications of Ce-NiO

1. Electrochemical Biosensors

Ce-doped NiO nanoparticles are extensively applied in electrochemical biosensing systems because of their superior electron transfer properties and chemically active surface [76]. The Ce^{3+}/Ce^{4+} redox couple plays a significant role in facilitating electron mediation during electrochemical processes, thereby enhancing sensor sensitivity and reducing response time. In addition, Ce-induced oxygen vacancies provide numerous active adsorption sites for various analytes, including pesticides, glucose, and heavy metal ions [77]. The combined effect of improved charge transport and increased surface reactivity results in highly efficient detection of trace levels of substances, making Ce-doped NiO particularly valuable for environmental and biomedical sensing applications [78].

2. Gas Sensing Applications

Ce-doped NiO nanoparticles are widely recognized as efficient gas sensing materials due to their improved conductivity and enhanced surface reactivity. Interaction of target gases such as NO_2, NH_3, CO, and H_2S with the sensor surface results in measurable changes in resistance driven by electron-exchange mechanisms. The incorporation of cerium increases the concentration of oxygen vacancies, significantly enhancing gas adsorption capacity and strengthening surface interactions. Furthermore, the reversible Ce^{3+}/Ce^{4+} redox system supports rapid charge transfer and improves signal stability, resulting in faster response and recovery behavior suitable for environmental and industrial gas detection [66,71].

3. Photocatalytic Degradation of Pollutants

In photocatalytic systems, Ce-doped NiO nanoparticles exhibit improved performance in degrading organic contaminants, including dyes, pharmaceutical residues, and industrial effluents [74]. Cerium incorporation narrows the band gap of NiO, enabling better utilization of visible light and promoting the generation of electron–hole pairs. Moreover, Ce ions act as charge trapping centres through their redox cycling, thereby minimizing recombination losses. The generated charge carriers participate in surface reactions to form reactive oxygen species, including hydroxyl radicals (•OH) and superoxide radicals ($O_2^{\bullet -}$), which effectively decompose complex pollutants into environmentally safe products [72].

4. Energy Storage Devices (Supercapacitors and Batteries)

Ce-doped NiO nanoparticles are promising electrode materials for energy storage applications due to their enhanced electrochemical activity. The material exhibits pseudocapacitive behavior driven by reversible redox transitions between Ni^{2+}/Ni^{3+} and Ce^{3+}/Ce^{4+} states, which significantly contributes to charge storage capability [72]. Additionally, improved electrical conductivity along with a higher number of electroactive sites enables efficient ion diffusion and rapid electron transport during charge–discharge cycles. These characteristics result in higher capacitance, improved rate performance, and better long-term cycling stability, making them suitable for advanced energy storage technologies [74,77].

5. Electrocatalysis

Ce-doped NiO nanoparticles exhibit strong electrocatalytic properties owing to their defect- rich structure and modified electronic configuration. Oxygen vacancies, along with mixed valence states of cerium and nickel, provide abundant active centres that enhance electrochemical reaction kinetics [76]. These features make the material effective for key catalytic reactions such as the oxygen evolution reaction (OER) and the hydrogen evolution reaction (HER). The Ce^{3+}/Ce^{4+} redox pair further improves electron-transfer efficiency during catalytic processes, thereby lowering the activation energy and enhancing overall catalytic activity [75].

6. Environmental Monitoring and Remediation

Ce-doped NiO nanoparticles are widely employed in environmental monitoring and remediation due to their strong affinity toward pollutants and high surface reactivity. In sensing applications, even very low concentrations of contaminants can be detected through significant changes in electrical signals caused by surface charge interactions. In remediation processes, these nanoparticles contribute to the breakdown and removal of toxic organic and inorganic substances

from environmental matrices. This dual functionality makes them highly effective for sustainable water and air purification technologies [68,78].

7. Optoelectronic Applications

In optoelectronic devices, Ce-doped NiO nanoparticles are utilized because of their tunable electronic structure and enhanced light absorption properties [77]. The introduction of cerium creates defect energy levels within the band gap, thereby improving optical absorption and altering electronic transition behaviour. This facilitates better generation and transport of charge carriers. Moreover, enhanced separation of photoinduced electron–hole pairs lead to improved device efficiency and stability, making these materials suitable for photodetectors, photoelectrochemical systems, and other light-driven electronic applications [78,74].

References

1. H. Saad, S.A. Elfeky, N.E.A El-Gamel, and A.S. Abo Dena, A. S. (2025), Organophosphate pesticides: A review on classification, synthesis, toxicity, remediation and analysis, RSC Advances, 15:40802–40822.
2. M.A. Ghorab, and M. S. Khalil (2015), Toxicological Effects of Organophosphates Pesticides, International Journal of Environmental Monitoring and Analysis, 3:218–224.
3. M. Jokanovic (2018), Neurotoxic effects of organophosphorus pesticides and possible association with neurodegenerative diseases in man: A review, Toxicology, 410:125–131.
4. L.G. Costa (2006), Current issues in organophosphate toxicology, Clinica Chimica Acta, 366:1–13.
5. M. Eddleston, N.A. Buckley, P. Eyer, and A.H. Dawson (2008), Management of acute organophosphorus pesticide poisoning, The Lancet, 371: 597–607.
6. T.R. Fukuto (1990), Mechanism of action of organophosphorus and carbamate insecticides, Environmental Health Perspectives, 87:245–254.
7. D.M. Roberts, and C.K. Aaron (2007), Managing acute organophosphorus pesticide poisoning, BMJ, 334:629–634.
8. K.D. Racke (1993), Environmental fate of organophosphate pesticides, Reviews of Environmental Contamination and Toxicology, 131:1–150.
9. M.W. Aktar, D. Sengupta, and A. Chowdhury (2009), Impact of pesticides use in agriculture: Their Benefits and Hazards, Interdisciplinary Toxicology, 2:1–12.
10. C.S. Pundir, and N. Chauhan (2012), Acetylcholinesterase inhibition-based biosensors for pesticide determination: A review, Analytical Biochemistry, 429:19–31
11. M. Jokanovic (2018), Neurotoxic effects of organophosphorus pesticides and possible association with neurodegenerative diseases in man: A review, Toxicology, 410:125–131.
12. J.V. Peter, T.I. Sudarsan, and J.L. Moran (2014), Clinical Features of Organophosphate Poisoning: A Review, Current Opinion in Critical Care, 20:143–150
13. J. Mearns, J. Dunn, and P.R. Lees-Haley (1994), Psychological effects of organophosphate pesticides: A review and call for research, Journal of Clinical Psychology, 50:286–294
14. L. Karalliedde, and N. Senanayake (1989). Organophosphorus Insecticide Poisoning, British Journal of Anaesthesia, 63:736–750
15. M.A. Ghorab, and M.S. Khalil (2015), Toxicological Effects of Organophosphates Pesticides, International Journal of Environmental Monitoring and Analysis, 3:218–224.
16. P. Eyer (2003), The Role of Oximes in the Management of Organophosphorus Pesticide

Poisoning. Toxicological Reviews, 22:165–190.

17. N. Senanayake, and L. Karalliedde (1987), Neurotoxic effects of organophosphorus insecticides: An intermediate syndrome, New England Journal of Medicine, 316:761–763.

18. M.B. Detweiler (2012), Organophosphate intermediate syndrome with neurological complications of extrapyramidal symptoms in clinical practice, Primary Care Companion for CNS Disorders, 14:11l01345

19. J.L. De Bleecker, K. Van den Neucker, J.L. Willems, and D. Lison (1993), The intermediate syndrome in organophosphate poisoning: A prospective study, Critical Care Medicine, 21: 1706–1711.

20. M.K. Johnson (1975), Organophosphorus esters causing delayed neurotoxic effects: Mechanism of action and structure–activity relationships, Critical Reviews in Toxicology, 3:289–316.

21. M. Lotti (2001), Clinical toxicology of anticholinesterase agents in humans, In Handbook of Pesticide Toxicology (2nd ed.), Academic Press, 2:1043–1085.

22. M.B. Abou-Donia (2003), Organophosphorus ester-induced chronic neurotoxicity, Archives of Environmental Health, 58:484–497.

23. M. Lotti, and A. Moretto (2005), Organophosphate-induced delayed polyneuropathy, Toxicological Reviews, 24:37–49.

24. M. Jokanovic, and M. Kosanovic (2010), Neurotoxic effects in patients poisoned with organophosphorus pesticides, Environmental Toxicology and Pharmacology, 29:195–201

25. D.S. Rohlman, W.K. Anger, P.J. Lein, and L.A. Corral (2011), Neurobehavioral performance in agricultural and pesticide workers, NeuroToxicology, 32:490–498.

26. M.B. Abou-Donia (2003), Organophosphorus ester-induced chronic neurotoxicity, Archives of Environmental Health, 58:484–497.

27. Y. Chen, Z. Yang, B. Nian, C. Yu, D. Maimaiti, M. Chai, X. Yang, X. Zang, and D. Xu (2024), Mechanisms of neurotoxicity of organophosphate pesticides and their relation to neurological disorders, Neuropsychiatric Disease and Treatment, 20:1535–1558.

28. V. Kumar, N. Upadhay, A.B. Wasit, S. Singh, and P. Kaur (2023), Spectroscopic Methods for the Detection of Organophosphate Pesticides – A Preview, Journal of Environmental and Analytical Toxicology, 8:313.

29. M. Bhattu, M. Verma, and D. Kathuria (2021), Recent advancements in the detection of organophosphate pesticides: A review, Analytical Methods, 13:4390–4428.

30. H. John, and H. Thiermann (2021), Poisoning by organophosphorus nerve agents and pesticides: An overview of the principle strategies and current progress of mass spectrometry-

based procedures for verification, Journal of Mass Spectrometry and Advances in the Clinical Lab, 22:39–53.

31. N. Majidiyan, S.P. Mousavi, and M.F Vajargah (2025), Assessing the impact of organophosphorus pesticides (OPPs) on aquatic ecosystems: A review, Journal of New Medical Innovations and Research, 6:1-14.

32. B. Fei-Baffoe, K.A. Dankwah, A. Sangber-Dery, E.E.Y. Amuah, and L.N.A Sackey (2024), Evaluation and implications of organophosphate pesticide residues in cabbage (Brassica oleracea), Heliyon, 10:37962.

33. J.A. Dahl, B.L.S. Maddux, and J.E. Hutchison (2007), Towards greener nanosynthesis. Chemical Reviews, 107:2228–2269.

34. M. Rai, A. Yadav, and A. Gade (2009), Silver nanoparticles as a new generation of antimicrobials, Biotechnology Advances, 27:76–83.

35. G. Aragay, and A. Merkoci (2012), Nanomaterials application in electrochemical detection systems, Chemical Communications, 48:531–549.

36. S. Chatterjee, H. Singh, D. Hudda, Sweety, and D. Kumar (2024), A Novel Acetylcholinesterase-Based Electrochemical Biosensor Using g-C_3N_4@MoS_2 Nanohybrid for the Detection of Trichlorfon, Applied Organometallic Chemistry, 38:7721.

37. S. Paneru, and D. Kumar (2023), Ag@ CuO Nanohybrid-Based Electrochemical Biosensor for Trichlorfon Detection, International Conference on Nanotechnology: Opportunities and Challenges, Springer, 28:75–84.

38. S. Li, J. Luo, Y. Wu, X. Ma, C. Pang, M. Wang, J. Luo, C. Zhang, and G. Tan (2022), Determination of trichlorfon using a molecularly imprinted electrochemiluminescence sensor on multi-walled carbon nanotubes decorated with silver nanoparticles, Microchimica Acta, 189:347.

39. W. Gao, F. Wan, W. Ni, S. Wang, M. Zhang, and J. Yu (2012), Electrochemical Sensor for Detection of Trichlorfon Based on Molecularly Imprinted Sol-Gel Films Modified Glassy Carbon Electrode, Journal of Inorganic and Organometallic Polymers and Materials, 22:37–41.

40. D. Zhao, Z. Yan, and X. Xiao (2025), Peroxidase-mimetic carbon dot based nanozyme hydrogel colorimetric sensor for visual trichlorfon detection, Spectrochimica Acta - Part A: Molecular and Biomolecular Spectroscopy, 336:126027.

41. L. Zhang, Q. Zhao, X. Tu, X. Yang, X. Lv, and S. Xiong (2025), Heterojunction of CuS/MnS Employed with Multiwalled Carbon Nanotubes in Molecularly Imprinted Sensor for Selective and Sensitive Determination of Trichlorfon Residual, Electroanalysis, 37:70086.

42. A. Banerjee et al. (2021), Nanotechnology for biosensors: A review, 21:1253.

43. Q. Tang, X. Shi, X. Hou, J. Zhou, and Z. Xu (2014), Development of molecularly imprinted electrochemical sensors based on Fe_3O_4@MWNT-COOH/CS nanocomposite layers for detecting traces of acephate and trichlorfon, Analyst (RSC), 139:6406–6413.

44. G. Aragay, and A. Merkoci (2012), Nanomaterials application in electrochemical detection systems, Chemical Communications, 48:531–549.

45. F. Dong, Z. Wang, Y. Sun, W.K. Ho, and H. Zhang (2017), Engineering 2D graphitic carbon nitride (g-C_3N_4) for photocatalysis and biosensing applications. Chemical Society Reviews, 46:1413–1432.

46. X. Wang, K. Maeda, A. Thomas, K. Takanabe, G. Xin, J.M. Carlsson, K. Domen, and M. Antonietti (2009), A metal-free polymeric photocatalyst for hydrogen production from water under visible light, Nature Materials, 8:76–80.

47. F. Dong, L. Wu, Y. Sun, M. Fu, Z. Wu, and S.C. Lee (2015), Efficient synthesis of polymeric g-C_3N_4 layered materials as novel efficient visible light driven photocatalysts, Journal of Materials Chemistry, 21:15171–15174.

48. J. Zhang, Y. Chen, and X. Wang (2015), Two-dimensional covalent carbon nitride nanosheets: Synthesis and energy applications, Advanced Materials, 27:757–762.

49. X. Li, J. Zhang, J. Shen, and H. Xu (2019), Graphitic carbon nitride-based nanomaterials for biomedical applications, Biomaterials Science, 7:453–466.

50. D. Zhao, C.L. Dong, B. Wang, C. Chen, Y.C. Huang, and S. Shen (2019), Z-scheme photocatalytic systems and g-C_3N_4 based sensors for environmental applications, Journal of Catalysis, 377:21–30.

51. Y. Zhang, T. Mori, L. Niu, and J. Ye (2011), Non-covalent functionalization of carbon nanotubes by conjugated polymers for flexible electronics, Nature Materials, 10:865–872.

52. Y. Wang, X. Wang, and M. Antonietti (2012), Polymeric graphitic carbon nitride as a heterogeneous photocatalyst for hydrogen evolution and CO_2 reduction, Angewandte Chemie International Edition, 51:68–89.

53. A. Banu, B. Sinha, and S. Sikdar, Synthesis of polymeric 2D-graphitic carbon nitride (g- C_3N_4) nanosheets for sustainable photodegradation of organic pollutants, Heliyon, 10:33354.

54. X. Li, J. Zhang, J. Shen, and H. Xu (2019), Graphitic carbon nitride-based nanomaterials for biomedical and biosensing applications, Biomaterials Science, 7:453–466.

55. H. Liu, X. Wang, H. Wang, and R. Nie (2019), Graphitic carbon nitride quantum dots for biomedical applications: Recent advances and future perspectives, Journal of Materials

Chemistry B. 7:5432-5448.

56. S. Vinoth, K.S. Shalini Devi and A. Pandikumar (2021), A comprehensive review on graphitic carbon nitride based electrochemical and biosensors for environmental and healthcare applications, TrAC Trends in Analytical Chemistry, 140:116274.

57. R. Roy, A.R. Chacko, T. Abraham, B.K. Korah, B. K. John, M.S. Punnoose, C. Mohan, and B. Mathew (2022), Recent advances in graphitic carbon nitrides (g-C_3N_4) as photoluminescence sensing probe: A review, ChemistrySelect, 7:e202200876.

58. D. Bhanderi, P. Lakhani, and C.K. Modi (2023), Graphitic carbon nitride (g-C_3N_4) as an emerging photocatalyst for sustainable environmental applications: a comprehensive review, Sustainable Energy & Fuels, 7:4861-4894.

59. Q. Wang, Y. Li, F. Huang, S. Song, G. Ai, X. Xin, B. Zhao, Y. Zheng, and Z. Zhang (2022), Recent advances in g-C_3N_4-based materials and their application in energy and environmental sustainability, Frontiers in Chemistry, 10:1057478.

60. X. Yang, J. Peng, L. Zhao, H. Zhang, J. Li, P. Yu, Y. Fan, J. Wang, H. Liu, and S.X. Dou (2024), Insights on advanced g-C_3N_4 in energy storage: Applications, challenges, and future, Carbon Energy, 6:e490.

61. M.X. Liu, J.Y. Zhang, and X.L. Zhang (2022), Application of graphitic carbon nitride in the field of biomedicine: Latest progress and challenge, Materials Chemistry and Physics, 287:126325.

62. A. Alaghmandfard, and K. Ghandi (2022), A comprehensive review of graphitic carbon nitride (g-C_3N_4)–metal oxide-based nanocomposites: Potential for photocatalysis and sensing, Nanomaterials, 12:294.

63. R. Sivakumar, and V. Rajendran (2013), Electrical and sensing properties of rare-earth doped NiO nanostructures, Superlattices and Microstructures, 60:412–420.

64. F. Dong, Z. Wang, Y. Sun, W.K. Ho, and H. Zhang (2017), Engineering graphitic carbon nitride (g-C_3N_4) based nanocomposites for photocatalytic applications, Chemical Society Reviews, 46:1413–1432.

65. S. Kumar, and R. Singh (2016), Metal oxide nanostructures for electrochemical sensing applications, Sensors and Actuators B: Chemical, 223:111–126.

66. T. Prakash, and R. Jayaprakash (2016), Electrochemical performance of Ce-doped NiO nanostructures, Electrochimica Acta, 190:386–393.

67. K.R. Reddy, K. Karthik, S.B.B. Prasad, R. Soni, and N.P. Shetti (2019), Nanostructured metal oxide-based materials for electrochemical applications: A review, Journal of Electroanalytical Chemistry, 847:113203.

68. A. Sharma, M. Varshney, and K.H. Chae (2018), Influence of rare-earth doping on structural, optical and electronic properties of metal oxide nanostructures, Journal of Alloys and Compounds, 740:129–136.

69. P. Gao, M. Sun, and Y. Wang (2020), Rare-earth doped metal oxide nanomaterials: synthesis and morphology control, Ceramics International, 46:12345–12356

70. R. Elilarassi, and G. Chandrasekaran (2010), Structural, optical and magnetic studies on Ce-doped NiO nanoparticles, Journal of Materials Science: Materials in Electronics, 21:1167–1173.

71. D. Zhao, C.L. Dong, B. Wang, C. Chen, Y.C. Huang, and S. Shen (2019), Synergy of defect engineering and heterojunction construction in photocatalytic materials: Recent advances and perspectives, Journal of Catalysis, 377:21–30.

72. G. Aragay, and A. Merkoci (2012), Nanomaterials application in electrochemical detection systems, Chemical Communications, 48:531–549.

73. K. Karthik, S. Dhanuskodi, and C. Gobinath (2017), Enhanced photocatalytic and antibacterial activity of Ce-doped NiO nanoparticles, Journal of Photochemistry and Photobiology B: Biology, 173:209–216.

74. S.M. Sze, and K.K. Ng (2006), Physics of Semiconductor Devices (3rd ed.), Wiley.

75. S. Muthukumaran, and R. Gopalakrishnan (2012), Gas sensing properties of Ce-doped NiO nanoparticles, Materials Letters, 72:123–126.

76. K.K. Bharathi, and H. John (2019), Optical and photoelectrochemical properties of Ce- doped NiO nanoparticles, Materials Science in Semiconductor Processing, 93:191–198.

77. G. Wang, L. Zhang, and J. Zhang (2012), A review of electrode materials for electrochemical supercapacitors, Chemical Society Reviews, 41:797–828.

78. P. Simon, and Y. Gogotsi (2008), Materials for electrochemical capacitors, Nature Materials, 7:845–854.

Chapter – 3

Materials and Methods

3.1 Introduction

This unit introduces the materials Ce-doped NiO and graphitic carbon nitride, produces their nanoparticles, and characterizes them using different techniques, including electrochemical techniques and morphological studies, for the fabrication of biosensors for the analysis of organophosphate pesticides. This unit also discusses the parameters, methodologies, and protocols associated with the development and performance efficiency of biosensors.

3.2 Materials

The description of each material used is given as follows:

3.2.1 Chemicals

Nickel nitrate hexahydrate [$Ni(NO_3)_2.6H_2O$], Cerium nitrate hexahydrate [$Ce(NO_3)_3.6H_2O$], Ascorbic acid (AA; 99%), Glucose ($C_6H_{12}O_6$; ≥ 99.5%), Uric acid (UA; ≥ 99%) and Sodium chloride (NaCl), Potassium chloride (KCl), Zinc sulphate (Zn_2SO_4), Acetylcholinesterase (AChE), Acetylthiocholine chloride (ATCl), Trichlorfon (TF) and Glutaraldehyde solution were taken from Sigma-Aldrich. Acetone, ethanol, and hydrochloric acid (HCl) were used as solvents, and for real-sample analysis, we used rice, apple, and cucumber. All reagents used in the synthesis were of analytical grade and employed without auxiliary purification.

3.2.2 Solutions and Buffer

- Phosphate buffer saline (PBS;0.1 M) having pH 7,
- 5mM $[Fe(CN)_6]^{3-/4-}$ used in PBS solution as redox initiator.

3.3 Characterization Techniques

With the help of a three-phase electrode system, characterization of synthesized nanoparticles of the material to determine its structural properties is done using various techniques such as X-ray diffraction (XRD) and Fourier transform infrared spectroscopy (FTIR). For morphological and elemental characterization technique used is Field-emission electron microscopy (FE-SEM). Electrochemical analysis was performed through cyclic voltammetry (CV) and differential pulse

voltammetry (DPV).

3.3.1 X-Ray Diffraction (XRD)

X-ray diffraction (XRD) is a highly effective, non-destructive analytical technique widely used to investigate crystalline materials. It yields detailed insights into crystal structure, phase identification, preferred orientation (texture), and structural parameters such as crystallite size, degree of crystallinity, lattice distortion, and structural defects [1]. The diffraction pattern results from the constructive interference of monochromatic X-rays reflected from regularly spaced lattice planes at specific diffraction angles. The intensity of the diffraction peaks is governed by the arrangement of atoms in the crystal lattice. As a result, an XRD pattern serves as a unique signature of the material's periodic atomic structure [2].

A more effective introduction to the application of X-ray diffraction in determining crystal structures can be presented through a simplified model. Typically, the explanation starts with a diagram illustrating an ordered arrangement of scattering points positioned along parallel planes separated by a distance *d,* shown in (**Fig. 3.1**). The interaction of X-ray beams with these planes is then examined, where the rays are reflected in a manner similar to mirror reflection.

Constructive interference takes place when the difference in path length between X-rays reflected from adjacent crystal planes is equal to an integral multiple (n) of the X-ray wavelength. This condition directly results in Bragg's law:

$$n\lambda = 2d\sin\,\theta$$

where λ corresponds to the wavelength of generated X-rays, θ denotes the angle formed between the surface of the reflecting crystalline lattice and the incident ray [3].

XRD provides precise information about crystal structure, phase identification, and lattice parameters. The method requires minimal sample preparation and can deliver rapid results with high accuracy and reproducibility. Additionally, it can analyze a wide range of materials, including powders, thin films, and bulk solids [4].

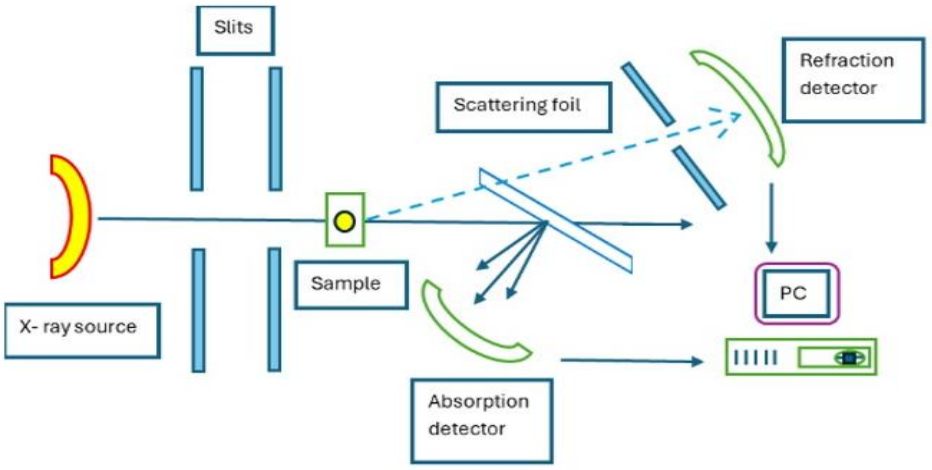

Fig. 3.1 Schematic Diagram of X-Ray Diffractometer

3.3.2 Fourier Transform Infrared Spectroscopy (FTIR)

IR spectroscopy is widely employed to analyze molecular vibrational modes, with each functional group exhibiting distinct absorption bands within the infrared region, which are associated with their fundamental vibrational motions [5]. For a nonlinear molecule containing N atoms, the total number of possible vibrational modes is given by $3N - 6$, representing the independent ways in which the atoms can move. For a molecular vibration to be IR active, it must be accompanied by a variation in the molecule's dipole moment. Consequently, symmetric vibrations are generally not observed in IR spectra, especially in molecules that possess a centre of symmetry, where such vibrations remain inactive [6]. On the other hand, asymmetric vibrations are typically IR active and can be detected. This broad sensitivity enables IR spectroscopy to analyze a wide variety of chemical groups within a single sample, including substances such as amino acids and water, which are often difficult to study with other techniques. Strong infrared absorption is usually associated with polar bonds that have a permanent dipole moment. Within the mid-infrared region (4000–1000 cm^{-1}), the spectra are primarily characterized by two types of molecular vibrations, namely stretching vibrations (ν) and bending vibrations, which involve changes in bond length, and bending vibrations, which involve variations in bond angles [7]. Bending vibrations can occur either in the plane (δ) or out of the plane (π) of the molecule. Stretching vibrations are commonly described using the harmonic oscillator model, in which a chemical bond is treated as a system of two masses connected by a spring. In this model, the bond strength is represented by the force constant (k), while the masses (m_1 and m_2) correspond to the atoms or groups forming the bond. The vibration frequency(ν), which depends on both the bond strength and the masses of the atoms

involved, is determined using

$$\nu = (1/2\pi c)\sqrt{k(m1 + m2)/m1m2}$$

Fourier Transform Infrared (FTIR) spectroscopy is an advanced analytical method used to identify chemical compounds and study molecular structures by measuring their infrared absorption spectra [8]. Unlike conventional infrared spectroscopy, FTIR simultaneously collects all infrared wavelengths, resulting in faster data acquisition and improved signal quality. The technique operates by transmitting a broad range of infrared radiation through a sample and recording the frequencies absorbed by the material, which correspond to specific molecular vibrations of chemical bonds [9]. The resulting absorption patterns generate a characteristic spectral fingerprint that enables the identification of specific functional groups within a sample and analyzes the material composition. All this was done using a Michelson interferometer, as shown in (**Fig. 3.2**). FTIR requires little to no sample preparation and can be used for the analysis of solids, liquids, and gases, making it a versatile tool in fields such as chemistry, material science, pharmaceuticals, and environmental analysis [10].

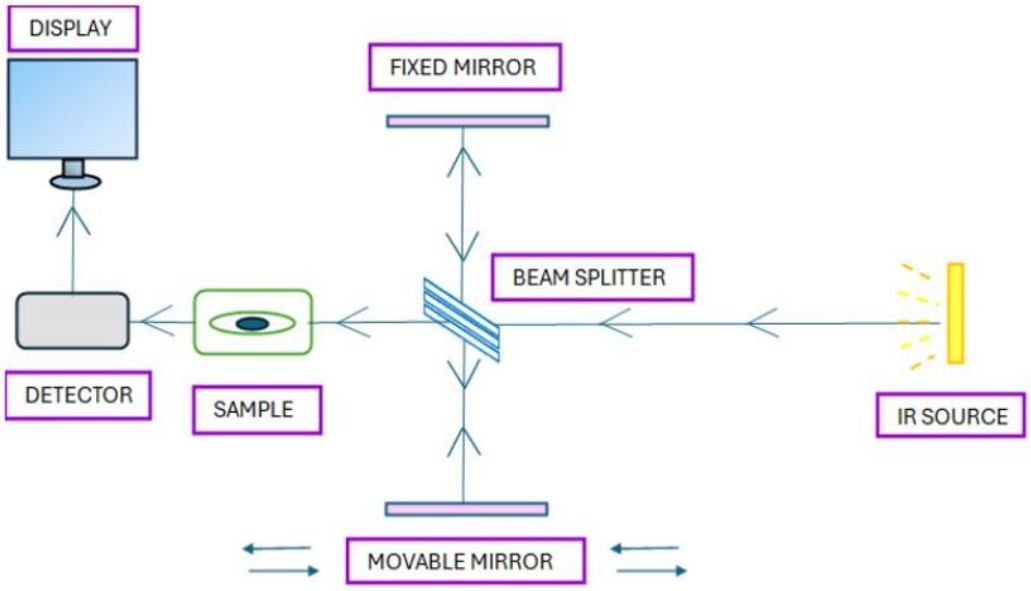

Fig. 3.2 Schematic Diagram of the Michelson Interferometer

3.3.3 Scanning Electron Microscopy (SEM)

Scanning electron microscopy (SEM) is a versatile analytical technique widely used to examine the microstructural morphology and chemical composition of materials [11]. SEM technique operates by directing a beam of high-energy electrons onto the sample surface, where electron–matter interactions generate various detectable signals that are converted into detailed images [12]. Understanding the basic principles of light optics is essential for grasping the fundamentals of electron microscopy. SEM is widely used across disciplines, including materials science, biological research, and nanotechnology, because it provides clear insight into microstructural characteristics that are not visible with conventional optical microscopes [13].

The resolution limit refers to the smallest distance at which two separate features can still be distinguished as individual entities. According to Ernst Abbe, the resolving power of an imaging system is directly influenced by the wavelength of the illuminating radiation [14]. When the resolution surpasses this limit at a given wavelength, the enlarged image becomes indistinct.

Due to diffraction and interference effects, light originating from a point source cannot be focused into an exact point; instead, it appears spread out [15].

Resolution in an ideal optical system can be expressed mathematically using Abbe's equation:

$$d = \frac{0.612\lambda}{n\sin\alpha}$$

Here:

- d represents the resolving power (minimum distinguishable distance)
- λ represents the wavelength of the radiation used for imaging
- n represents the refractive index of the medium separating the specimen and the objective lens, measured relative to free space
- α denotes the half of the angular aperture of the cone of light entering the objective lens (measured in radians)

The quantity n sin α is known as the numerical aperture (NA), a parameter that describes the light-gathering capability of an optical system. [16].

One of the most significant features of SEM is its capability to produce high-resolution surface images with excellent depth-of-field control, giving the sample surface a three-dimensional appearance. It also enables detailed surface analysis and can be combined with techniques such as elemental analysis to determine chemical composition. Additionally, SEM can examine a wide range of materials with minimal sample preparation, enhancing its versatility and effectiveness in scientific research and industrial applications [17].

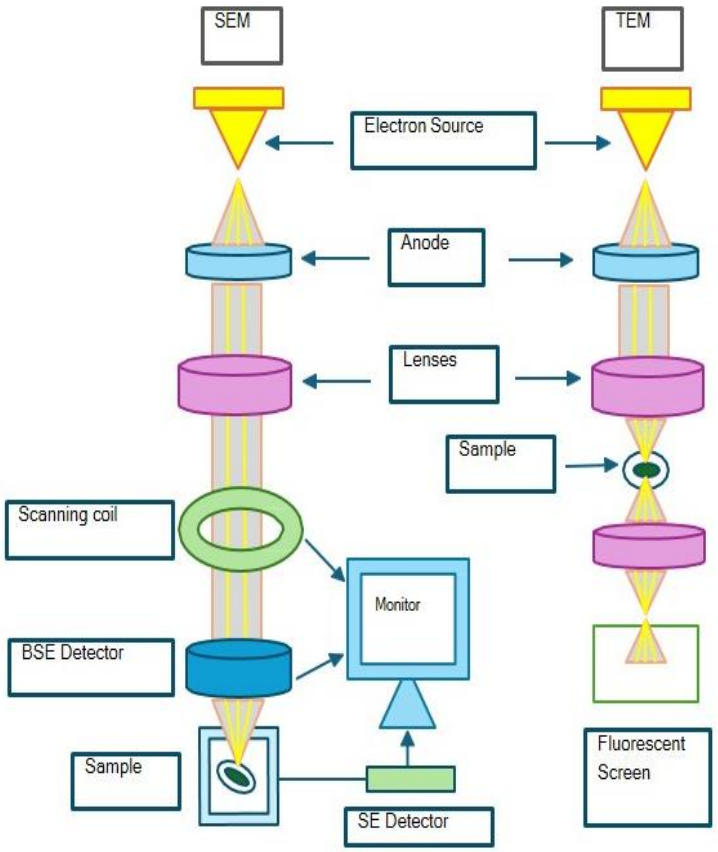

Fig. 3.3 Schematic Diagram of Scanning Electron Microscopy (SEM) and Transmission Electron Microscopy (TEM)

3.4 Electrochemical Techniques

Electrochemical methods rely on electrochemical principles to investigate chemical reactions, substance concentrations, and physicochemical properties [18]. These approaches have certain advantages over surface-modification techniques because they exploit the interaction between electric current and chemical species at the electrode-electrolyte interface. Such methods typically involve at least three components: electrodes, an electrolyte solution, and an external electrical circuit [19]. In this work, a three-electrode setup comprising a reference electrode (Ag/AgCl), a platinum counter electrode, and a working electrode is connected to a potentiostat (an Autolab (Ecochemie, Netherlands) Galvanostat/Potentiostat) [20]. The instrument regulates the potential applied to the working electrode and records the corresponding current response, generating a plot of current versus time. A schematic of the potentiostat configuration is illustrated in (**Fig. 3.4**). Common electrochemical techniques employed include Differential Pulse Voltammetry (DPV), Cyclic Voltammetry (CV), Electrochemical Impedance Spectroscopy (EIS), and Chronoamperometry [21].

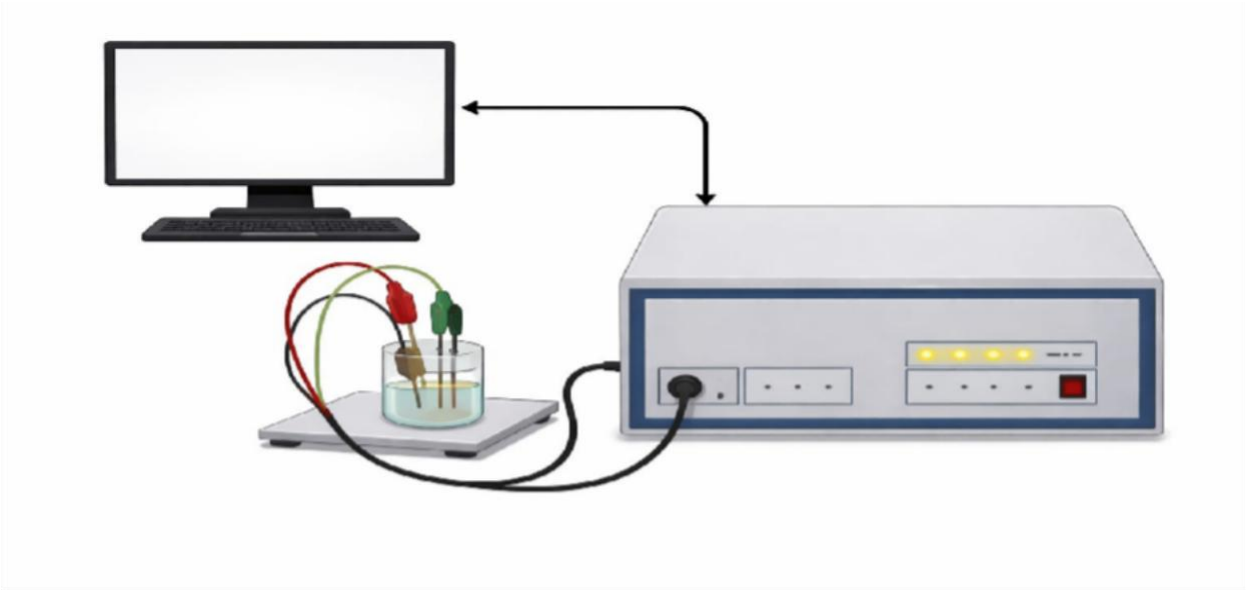

Fig. 3.4 Schematic Diagram of the Potentiostat

3.4.1 Differential Pulse Voltammetry (DPV)

Differential pulse voltammetry (DPV) is an electroanalytical technique known for its high sensitivity used to detect and quantify low-concentration redox-active species by minimizing background capacitive (charging) currents [22]. In DPV, a potential scan is carried out as a staircase or linear ramp, with small, constant-amplitude potential pulses (typically 10-100 mV) superimposed at regular intervals on each step. In each pulse cycle, the current is sampled at two points—just prior to the application of the pulse and at its termination. The difference in current between the two measurements is plotted as a function of the applied potential, yielding a peak-shaped voltammogram [23, 24]. This differential measurement suppresses the contribution of non-faradaic charging current, thereby greatly improving the signal-to-noise ratio and facilitating the detection of analytes at extremely low concentrations, often in the nanomolar range [21].

The peak height in a DPV voltammogram is generally proportional to the concentration of the electroactive species, enabling the construction of calibration curves for quantitative analysis, while the peak potential provides information about the effective half-wave potential and redox behaviour of the system [22]. Reversible processes typically give symmetric, well-defined peaks, whereas irreversible or adsorption-controlled reactions may produce broader or asymmetric features.

DPV also offers good resolution among multiple redox couples because differential measurement

reduces background capacitive current and emphasizes faradaic contributions that change rapidly with potential [23]. This allows discrimination of closely spaced oxidation or reduction events that might overlap in conventional linear-sweep or cyclic voltammetry. Further control parameters such as pulse amplitude, pulse width, step size, and scan rate can be optimized to balance sensitivity, resolution, and analysis time [25, 26]. Due to these advantages, DPV is widely used in trace analysis of heavy metals, pharmaceuticals, and environmental pollutants, as well as in biosensing platforms, modified-electrode characterization, and the study of electrocatalytic mechanisms on nanomaterials and functionalized surfaces [23].

3.4.2 Cyclic Voltammetry (CV)

Cyclic voltammetry (CV) is an electrochemical method employed to study the redox behaviour and reaction mechanisms of chemical species in solution or at an electrode surface [22]. In a typical cyclic voltammetry (CV) experiment, the working electrode potential is swept linearly with time between two predefined limits using a triangular waveform, while the resulting current is continuously measured and plotted against the applied potential to obtain a cyclic voltammogram [23]. This technique is typically performed using a three-electrode setup comprising of a working electrode, a reference electrode, and a counter electrode, with the potential controlled by a potentiostat [24]. Analysis of peak positions, peak separation, and peak currents allows determination of parameters such as formal redox potentials, reversibility of electron-transfer processes, number of electrons involved, diffusion coefficients, and surface coverage of electroactive species [22]. Because of its simplicity, sensitivity, and ability to provide rapid qualitative and semi-quantitative information.

In cyclic voltammetry (CV) voltammograms, peak currents and peak-to-peak separations provide key information about the electrochemical behaviour of the species under study [27]. The anodic peak current (i_{pa}) and cathodic peak current (i_{pc}) are proportional to the concentration of the electroactive species and the scan rate, with reversible systems following the Randles-Ševčík relationship such that $i_p \propto \nu$, where ν is the scan rate [28]. By plotting the peak current against the square root of the scan rate, one can distinguish between diffusion-controlled and adsorption-controlled processes and estimate diffusion coefficients. The Randles-Ševčík equation:

$$i_p = (2.69 \times 10^5)\, n^{3/2} A D^{1/2} C \nu^{1/2}$$

where n represents the number of electrons involved in the redox process, A denotes the electrode's surface area, D is the diffusion coefficient, C is the bulk analyte concentration, and ν represents

the scan rate [29,30].

This allows a clear, quantitative interpretation of the electroactive species' behaviour at the electrode–electrolyte interface and strengthens the mechanistic discussion [27]. CV is widely used in electrode characterization, catalysis, corrosion studies, sensor development, and the investigation of organic, inorganic, and polymeric electroactive materials [23].

3.4.3 Electrochemical Impedance Spectroscopy (EIS)

Electrochemical Impedance Spectroscopy (EIS) is a powerful frequency-domain method that examines the electrical response of an electrode–electrolyte interface by applying a low-amplitude sinusoidal potential across the wide frequency spectrum [31, 32]. The measured current or voltage response is analyzed in terms of impedance, which is expressed as a complex quantity consisting of a real (resistive) and an imaginary (capacitive or inductive) component [22]. EIS provides detailed information on interfacial processes, including charge-transfer resistance, double-layer capacitance, diffusion-controlled mass transport, and the presence of surface films or coatings, often represented by equivalent electrical circuits comprising resistors, capacitors, and other elements [33, 32].

Because EIS is performed under nearly non-perturbing conditions, it is particularly useful for studying corrosion mechanisms, battery electrode interfaces, fuel cells, supercapacitors, and biosensor platforms without significantly altering the system [34]. The resulting data are commonly visualized as Nyquist or Bode plots, from which key parameters such as polarization resistance, film resistance, and diffusion time constants can be extracted by fitting the spectra to appropriate models. In thesis work, EIS is frequently combined with techniques like cyclic voltammetry or chronoamperometry to correlate electrochemical behavior with interfacial structure and to monitor changes in electrode properties over time or under different experimental conditions [35, 32, 33].

In electrochemical studies, Electrochemical Impedance Spectroscopy (EIS) is an important non-destructive technique used to investigate both interfacial and bulk properties of electrochemical systems [34]. By applying a small-amplitude sinusoidal potential or current perturbation over a broad frequency range and measuring the complex impedance response, EIS enables the separation of contributions such as solution resistance, charge-transfer resistance, double-layer capacitance, and diffusion-controlled transport [35]. These processes are usually represented by an equivalent-circuit model, which is fitted to the experimental data (often displayed as Nyquist or Bode plots) to extract quantitative parameters like polarization resistance, film resistance, and diffusion time constants [32].

In this thesis, the EIS method is employed to determine the charge-transfer resistance (R_{ct}) from the measured EIS spectra. Equations (1) and (2) are then used to evaluate the exchange current density per unit geometric area (i_0) and the apparent electron-transfer rate constant (K_{app}) for different electrodes.

$$i_0 = \frac{nRT}{R_{ct}F} \qquad (1)$$

$$K_{\text{app}} = \frac{RT}{n^2F^2AR_{ct}C} \qquad (2)$$

Here, C represents the analyte concentration, F is Faraday's constant, A represents the electrode's geometrical surface area, n is the number of electrons participating in the redox process, T represents the absolute temperature, and R is the universal gas constant [35, 34].

Reference

1. V.K. Pecharsky, and P.Y. Zavalij (2009), Fundamentals of Powder Diffraction and Structural Characterization of Materials, Journal of Materials Science.
2. B.E. Warren (1990), X-ray Diffraction, Dover Publications.
3. A.A. Bunaciu, E.G. Udristioiu, and H.Y. Aboul-Enein (2015), X-Ray Diffraction: Instrumentation and Applications, Critical Reviews in Analytical Chemistry.
4. C.G Pope (1997), X-Ray Diffraction and the Bragg Equation, Journal of Chemical Education, 74: 129–131.
5. B. Stuart (2004), Infrared Spectroscopy: Fundamentals and Applications, Wiley.
6. C.N. Banwell, and E.M. McCash (1994), Fundamentals of Molecular Spectroscopy (4th ed.), McGraw-Hill.
7. D. Zhao, C.L. Dong, B. Wang, C. Chen, Y.C. Huang, and S. Shen (2019), Defect engineering in metal oxides for enhanced photocatalysis and sensing, Journal of Catalysis, 377: 21–30.
8. B.C. Smith (2011), Fundamentals of Fourier Transform Infrared Spectroscopy (2nd ed.), CRC Press.
9. P.R. Griffiths, and J.A. de Haseth (2007), Fourier Transform Infrared Spectrometry (2nd ed.), Wiley.
10. R.M. Silverstein, F.X. Webster, and D.J. Kiemle (2014), Spectrometric Identification of Organic Compounds (8th ed.), Wiley.
11. W. Zhou, R.P. Apkarian, Z.L. Wang, and D. Joy (2007), Fundamentals of Scanning Electron Microscopy, In Scanning Microscopy for Nanotechnology, Springer
12. J. Goldstein, D. Newbury, D. Joy, C. Lyman, P. Echlin, E. Lifshin, L. Sawyer, and J. Michael (2017), Scanning Electron Microscopy and X-ray Microanalysis (4th ed.), Springer.
13. L. Reimer (1998), Scanning Electron Microscopy: Physics of Image Formation and Microanalysis (2nd ed.), Springer.
14. E. Abbe (1873), Contributions to the Theory of the Microscope and the Nature of Microscopic Vision, Archiv fur Mikroskopische Anatomie, 9:413–418.
15. E. Hecht (2017), Optics (5th ed.), Pearson.
16. M. Born, and E. Wolf (1999), Principles of Optics: Electromagnetic Theory of Propagation, Interference and Diffraction of Light (7th ed.), Cambridge University Press.
17. R.F. Egerton (2005), Physical Principles of Electron Microscopy: An Introduction to TEM, SEM, and AEM, Springer.
18. A.J. Bard, and L.R. Faulkner (2001), Electrochemical Methods: Fundamentals and

Applications (2nd ed.), Wiley.

19. J. Wang (2006), Analytical Electrochemistry (3rd ed.), Wiley.

20. D.A. Skoog, F.J. Holler, and S.R. Crouch (2014), Principles of Instrumental Analysis (7th ed.), Cengage Learning.

21. F. Scholz (Ed.) (2010), Electroanalytical Methods: Guide to Experiments and Applications (2nd ed.), Springer.

22. G. Aragay, and A. Merkoci (2012), Nanomaterials application in electrochemical detection systems, Chemical Communications, 48:531–549.

23. K. Karthik, S. Dhanuskodi, and C. Gobinath (2017), Enhanced photocatalytic and antibacterial activity of Ce-doped NiO nanoparticles, Journal of Photochemistry and Photobiology B:Biology, 173:209–216.

24. B. Scrosati (1988), Electrochemical properties of conducting polymers, Progress in Solid State Chemistry, 18:1-77.

25. P.T. Kissinger, and W.R. Heineman (1983), Laboratory Techniques in Electroanalytical Chemistry, Marcel Dekker.

26. S. Malik et al. (2023), Nanomaterials-based biosensors and their applications, Heliyon, 9:e19929.

27. R.G. Compton, and C.E. Banks (2011), Understanding Voltammetry (2nd ed.), Imperial College Press.

28. R.S. Nicholson, and I. Shain (1964), Theory of Stationary Electrode Polarography**:** Single Scan and Cyclic Methods Applied to Reversible, Irreversible, and Kinetic Systems, Analytical Chemistry, 36:706–723.

29. J.E.B. Randles (1948), A Cathode Ray Polarograph, Transactions of the Faraday Society, 44:327–338.

30. A. Sevcik (1948), Oscillographic Polarography with Periodic Triangular Voltage, Collection of Czechoslovak Chemical Communications, 13: 349–377.

31. E. Barsoukov, and J.R. Macdonald (2005), Impedance Spectroscopy: Theory, Experiment, and Applications (2nd ed.), Wiley.

32. M.E. Orazem, and B. Tribollet (2008), Electrochemical Impedance Spectroscopy, Wiley.

33. B. Le, J. Khaliq, D. Huo, X. Teng, and I. Shyha (2020), A review on nanocomposites. Part 1: mechanical properties Journal of Manufacturing Science and Engineering, 142:100801.

34. A. Lasia (2014), Electrochemical Impedance Spectroscopy and its Applications, Springer.

35. A.J. Bard, and L.R. Faulkner (2001), Electrochemical Methods, Wiley.

Chapter – 4

Nickel-Cerium Oxide Decorated Graphitic Carbon Nitride-Based Electrochemical Biosensor for Organophosphate Pesticide Detection

4.1 Introduction

This chapter describes the development of a highly efficient acetylcholinesterase (AChE)-based electrochemical biosensor for detecting trichlorfon, incorporating a nanohybrid composed of graphitic carbon nitride (g-C_3N_4) and cerium-doped nickel oxide (Ce–NiO). The sensing mechanism relies on the inhibitory effect of trichlorfon, an organophosphate pesticide, on AChE activity, resulting in detectable changes in the electrochemical signal. The g-C_3N_4@Ce–NiO nanocomposite exhibits a pronounced synergistic effect due to the complementary characteristics of its constituents. Graphitic carbon nitride provides a high surface area, remarkable chemical stability, and numerous active sites for interaction, while cerium-doped nickel oxide offers enhanced electrical conductivity, superior redox activity, and improved catalytic performance due to the presence of Ce^{3+}/Ce^{4+} redox couples. This synergistic combination markedly increases the electroactive surface area, promotes faster electron transfer, and improves the overall electrocatalytic behaviour of the sensing platform. Moreover, the nanohybrid provides a biocompatible environment that supports effective immobilization and stability of AChE.

The biosensor was fabricated by modifying the electrode surface with the synthesized g-C_3N_4@Ce–NiO nanocomposite, followed by enzyme immobilization to create a sensitive bio-interface. Electrochemical characterization of the sensor was carried out using cyclic voltammetry (CV) and differential pulse voltammetry (DPV) to assess its performance. The resulting biosensor demonstrated excellent analytical characteristics, including high sensitivity (0.51 μA nM^{-1}), a low limit of detection (2.1 nM), and a wide linear range. It also exhibited strong selectivity toward trichlorfon in the presence of potential interfering species, along with good reproducibility and long-term stability.

Furthermore, the biosensor's applicability to real samples was confirmed by the successful detection of trichlorfon in three real samples. The obtained results showed satisfactory recovery rates and minimal interference from matrix components, indicating the reliability and robustness of the proposed sensing approach.

4.2 Experimental Section

4.2.1 Synthesis of g-C_3N_4 Nanosheets

Graphitic carbon nitride (g-C_3N_4) nanosheets were prepared via thermal condensation. In this procedure, 10 g of melamine was added to a covered crucible and subjected to calcination in the muffle furnace at 550 °C for 4 h. During this process, melamine underwent polymerization and condensation to form g-C_3N_4. The obtained yellowish product was thoroughly washed with distilled water and ethanol to remove residual impurities, then dried in a vacuum oven to yield the purified nanosheets.

4.2.2 Synthesis of Ce-NiO Nanoparticles

Cerium-doped nickel oxide (Ce–NiO) nanoparticles were synthesized using a co-precipitation method. Equimolar aqueous solutions (0.1 M) of nickel nitrate hexahydrate and cerium nitrate hexahydrate were prepared and mixed in 50 mL of deionized water under continuous stirring for 30 minutes. To maintain a pH of 10, 2 M NaOH was added gradually, resulting in the precipitation of the reaction product. The reaction mixture was stirred for an additional 3 h to ensure completion of the reaction. The resulting precipitate was collected and repeatedly washed with distilled water and ethanol to eliminate impurities. Subsequently, it was dried overnight in a vacuum oven at 60 °C and calcined at 400 °C for 3 h to obtain the final Ce–NiO nanoparticles.

4.2.3 Preparation of Ce-NiO@g-C_3N_4 Nanocomposite

The Ce–NiO@g-C_3N_4 nanocomposite was synthesized via a modified co-precipitation approach. Initially, 1.235 g of nickel nitrate hexahydrate was mixed in 10 mL of deionized water and stirred for 10 min to obtain a homogeneous solution. In a separate container, 0.3256 g of cerium nitrate hexahydrate was dissolved in 10 mL of deionized water under similar stirring conditions. The cerium precursor solution was gradually introduced into the nickel solution under continuous stirring. After adding 30 mL of distilled water, the mixture was stirred for a further 30 min. A sodium hydroxide solution, prepared by dissolving 2 g NaOH in 50 mL distilled water, was then added dropwise while monitoring the pH until it reached 10–11, leading to precipitate formation. The resulting mixture was stirred for an additional 3 h to ensure complete precipitation.

Afterwards, 250 mg of previously synthesized g-C_3N_4, dispersed in 50 mL of deionized water, was gradually incorporated into the reaction system under constant stirring. The resulting product was collected by filtration and thoroughly washed with a 1:1 mixture of distilled water and ethanol to remove residual impurities. The resulting product was vacuum-dried overnight at 60 °C, then

calcined at 400 °C for 3 h in a muffle furnace to yield the Ce–NiO@g-C_3N_4 nanocomposite.

4.2.4 Electrophoretic Deposition of Ce-NiO@g-C_3N_4 Nanocomposite

The prepared Ce–NiO@g-C_3N_4 composite was immobilized onto a pre-cleaned, hydrolyzed indium tin oxide (ITO) glass substrate (1.4 × 0.7 cm) through an electrophoretic deposition (EPD) process using a two-electrode setup. In this configuration, ITO functioned as the working electrode, whereas a platinum wire was utilized as the counter electrode, separated by approximately 1 cm. For the deposition, 0.5 mg of the nanocomposite was first dispersed in 15 mL of deionized water and subjected to ultrasonication to ensure a uniform and stable suspension. The deposition was then performed by applying a constant DC voltage of 10 V for 8 sec, yielding a thin, uniform nanohybrid film on the ITO surface.

4.2.5 Fabrication of Ce-NiO@g-C_3N_4 Nanohybrid- Based Biosensor

For biosensor fabrication, the Ce-NiO@g-C_3N_4/ITO modified electrode was first treated with 10 µL of 0.1% glutaraldehyde and maintained at room temperature for 60 min to enable cross- linking. Subsequently, 20 µL of acetylcholinesterase (AChE) solution (0.08 mg mL^{-1}, prepared in phosphate buffer solution at pH 7) was applied onto the electrode surface and allowed to incubate at 4°C for 12 h to ensure effective enzyme immobilization. Prior to electrochemical measurements, the electrode was rinsed with 50 µL of PBS to remove any loosely bound or unbound enzyme molecules.

4.3 Results and Discussion

4.3.1 Structural Characterization

Fig. 4.2 (A) represents the XRD patterns of g-C_3N_4, Ce-NiO and Ce-NiO@g-C_3N_4 nanocomposite in order to evaluate the crystalline characteristics of the synthesized materials. The diffraction peaks appearing at 2θ values of 37.1°, 43.3°, 62.7°, 75.3°, and 79.2° correspond to the (111), (200), (220), (311), and (222) planes, respectively **(curve b),** confirming the face-centered cubic structure of NiO. Upon cerium incorporation, the peak positions shift slightly toward lower angles and broaden, indicating lattice modification and defect generation due to successful doping. The presence of cerium oxide is indicated by low-intensity peaks appearing near 2θ values of 28.6°, 33.0°, 47.4°, and 56.3°, corresponding to its characteristic crystallographic planes. Characteristic peaks of g-C_3N_4 appear at 12.7° and 27.8°, associated with the (100) and (002) planes **(curve a)**.

In the composite, the presence of diffraction features from both g-C_3N_4 and Ce–NiO confirms the formation of a heterostructure. In the composite, the presence of diffraction features from both g-C_3N_4 and Ce–NiO, as represented by **curve c**, confirms the formation of a heterostructure. The reduced intensity of some peaks may result from overlap between NiO and g-C_3N_4 diffraction planes.

Fig. 4.2(B) displays the FT-IR spectra of g-C_3N_4, Ce-NiO, and Ce-NiO@g-C_3N_4. In the spectrum of g-C_3N_4, the broad absorption band extending from 1000 to 4000 cm^{-1} is characteristic of a graphitic framework, representing important vibrational modes including C=C stretching, C–H stretching, and O–H stretching. Specifically, the bands located at 1624 cm^{-1} and 3149cm^{-1} are attributed to sp^2 hybridized carbon and hydroxyl group, respectively. For the nanocomposite, the characteristic vibrational features of both g-C_3N_4 and CeO_2 remained observable. However, the absorption band corresponding to CeO_2 appears with reduced intensity in the nanocomposite, which may be due to its comparatively low content within the nanocomposite matrix. [18] Collectively, these FTIR features indicate the successful synthesis and effective structural integration of the Ce-doped NiO–g-C_3N_4 composite.

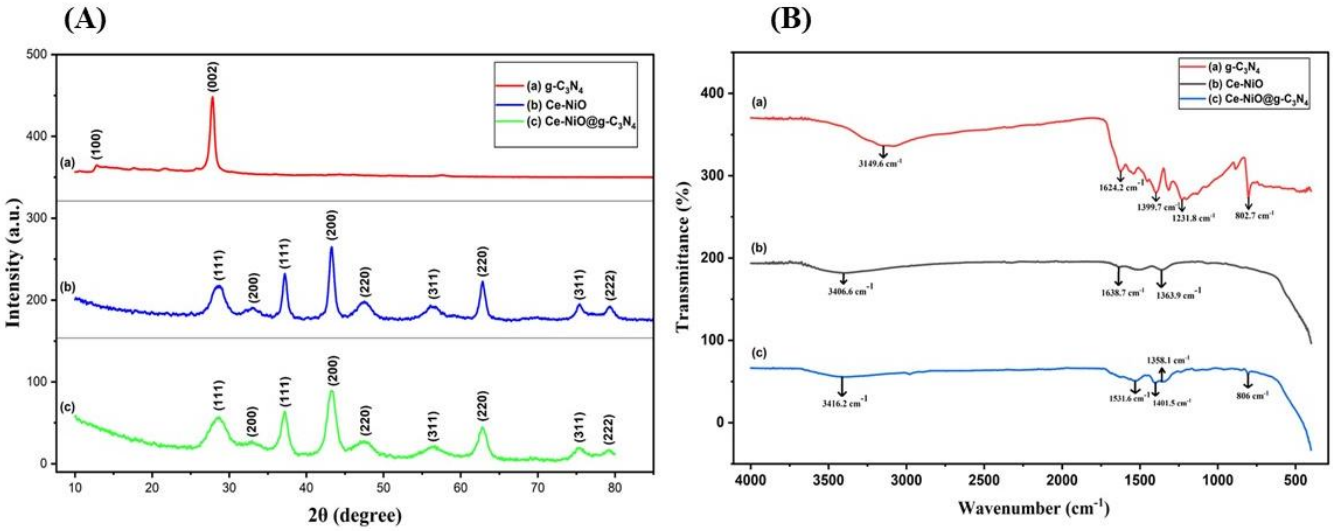

Fig. 4.2 (A) XRD and **(B)** FTIR of **(a)** g-C_3N_4, **(b)** Ce-NiO and **(c)** Ce-NiO@g-C_3N_4

4.3.2 Morphological Studies

The surface morphology of g-C_3N_4, Ce-NiO and Ce-NiO@g-C_3N_4 nanocomposite is analyzed using FE-SEM. As shown in **Fig. 4.3(A),** g-C_3N_4 shows a typical lamellar, sheet-like structure consisting of thin, irregularly stacked nanosheets. In **Fig. 4.3 (B)**, the Ce-doped NiO nanoparticles exhibit a spherical, sponge-like morphology with slight agglomeration and non-uniform particle size. The particles have a rough, porous surface with visible gaps. In **Fig.4.3 (C)**, the Ce-NiO@g-C_3N_4 nanocomposite shows a structure where spherical Ce-NiO nanoparticles are uniformly anchored on thin, sheet-like g-C_3N_4 layers.

The EDX spectrum of the Ce-NiO@g-C_3N_4 nanocomposite confirms its elemental composition and successful synthesis. The presence of C and N corresponds to the g-C_3N_4 matrix, while Ni and O peaks indicate the formation of NiO nanoparticles, as shown in **Fig. 4.3 (D)**. The appearance of Ce signals confirms successful cerium doping. Moreover, the absence of impurity peaks suggests high purity and effective integration of all components within the nanocomposite.

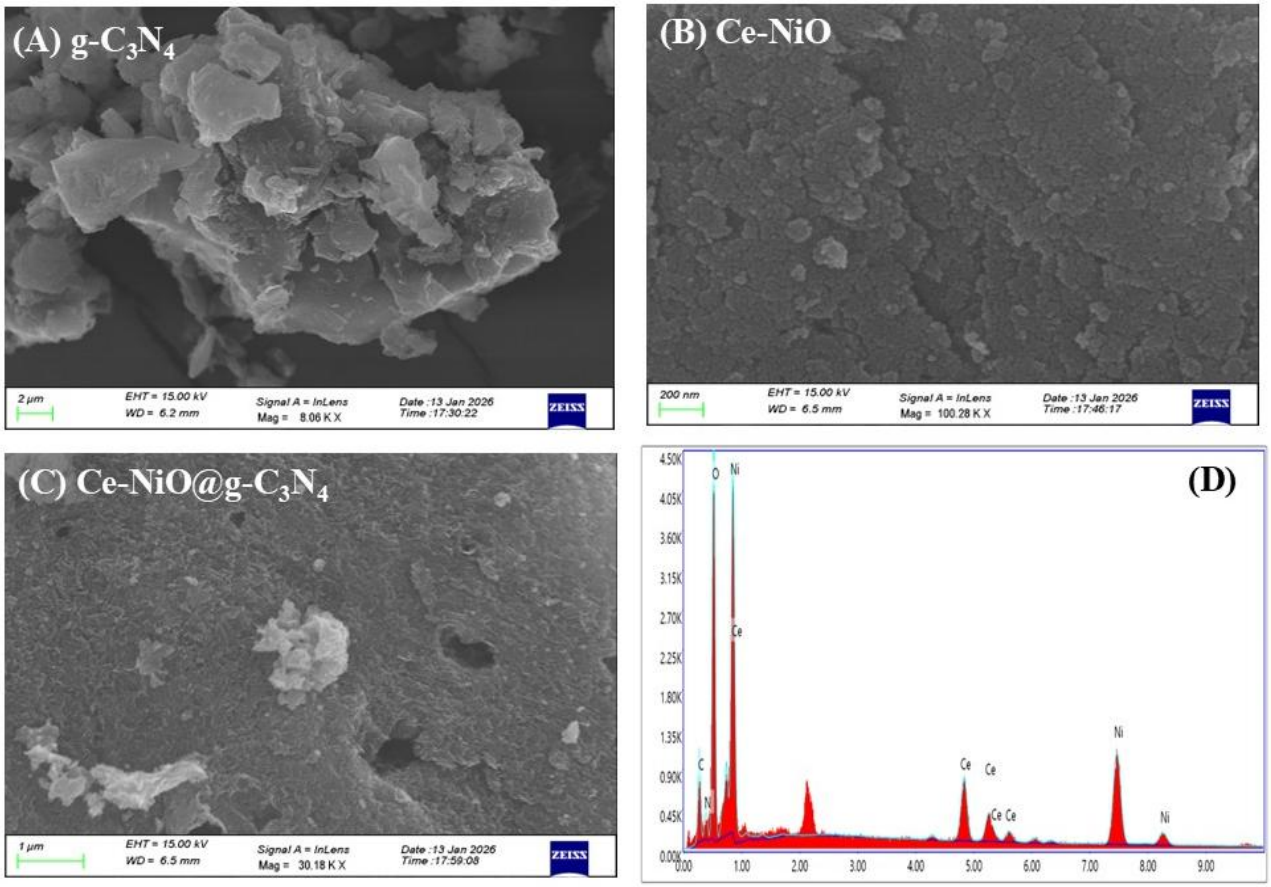

Fig. 4.3 FESEM images of **(A)** g-C_3N_4; **(B)** Ce-NiO; **(C)** Ce-NiO@g-C_3N_4; and **(D)** EDAX of Ce-NiO@g-C_3N_4

4.3.3 Electrochemical Characterization

The electrochemical performance of the fabricated electrodes was systematically evaluated using electrochemical impedance spectroscopy (EIS) and cyclic voltammetry (CV). The electron transfer resistance (R_{ct}) of all fabricated electrodes was evaluated using EIS in 0.2 M PBS consisting of 5 mM $[Fe(CN)_6]^{3-/4-}$ at an applied potential of 0.01 V over a frequency range of 0.01–10^5 Hz. From the Nyquist plot, a linear region at low frequencies was observed, representing the diffusion-controlled electron-transfer process, while a semicircular region at high frequencies corresponded to the charge-transfer process. The charge transfer resistance (R_{ct}) values for the modified electrodes were determined as 270 Ω for ITO **(curve a)**, 214 Ω for g- C_3N_4/ITO **(curve b)**, 169Ω for Ce-NiO/ITO **(curve c)**, 149 Ω for Ce-NiO@g-C_3N_4/ITO **(curve d)** and 176 Ω for AChE/Ce-NiO@g-C_3N_4/ITO **(curve e)**, respectively. The calculated exchange current density (i_o) values were found to be 11.999 × 10^{-5} and 17.234 × 10^{-5} A cm^{-2}, while the apparent electron transfer rate constants (K_{app}) were 5.076× 10^{-4} and 7.290× 10^{-4} cm s^{-1} for g-C_3N_4/ITO and Ce-NiO@g-C_3N_4/ITO, respectively, by using equations **4.1** and **4.2**.

$$i_0 = nRT/ R_{ct}F \qquad \textbf{4.1}$$

$$K_{app} = RT/n^2F^2AR_{ct}C \qquad \textbf{4.2}$$

Here, R, T, n, F, C, and A represent the gas constant, temperature, number of electrons, Faraday constant, concentration of $[Fe(CN)_6]^{3-/4-}$, and the electrode surface area, respectively. CV measurements were carried out at a scan rate of 50 mV/s for ITO, g-C_3N_4/ITO, Ce-NiO/ITO, Ce-NiO@g-C_3N_4 /ITO, and AChE/Ce-NiO@g-C_3N_4/ITO, as shown in **Fig.4.4 (B).** The Ce-NiO@g- C_3N_4 /ITO electrode **(curve d)** exhibited the highest peak current of 0.52 mA due to its large surface area and superior electrical conductivity as compared to g-C_3N_4/ITO **(curve b)** and Ce- NiO /ITO **(curve c),** which showed the current of 0.29 mA and 0.47 mA, respectively. On the other hand, the AChE-modified electrode (AChE/ Ce-NiO@g-C_3N_4/ITO) demonstrated reduced current response of 0.34 mA **(curve e)** due to the insulating nature of the enzyme, which restricts electron transfer.

The scan rate was 10-300 mV/s for Ce-NiO@g-C_3N_4/ITO (Fig. 4.4**(C))**. As the scan rate increased, the anodic peak potentials shifted toward more positive values, while the cathodic peak potentials shifted toward more negative values. Additionally, a linear relationship was observed between E_{pa} and E_{pc} and the logarithm of the scan rate (log ν) for Ce-NiO@g-C_3N_4/ITO (Fig. 4.4**(D))**, as

described by the following equations.

E_{pa} [Ce-NiO@g−C_3N_4/ITO] = 0.0808 (V) log (v) + 0.2024 (V); R^2 = 0.9797 **4.3**

E_{pc} [Ce-NiO@g−C_3N_4/ITO] = − 0.1026(V) log (v) + 0.2797 (V); R^2 = 0.9796 **4.4**

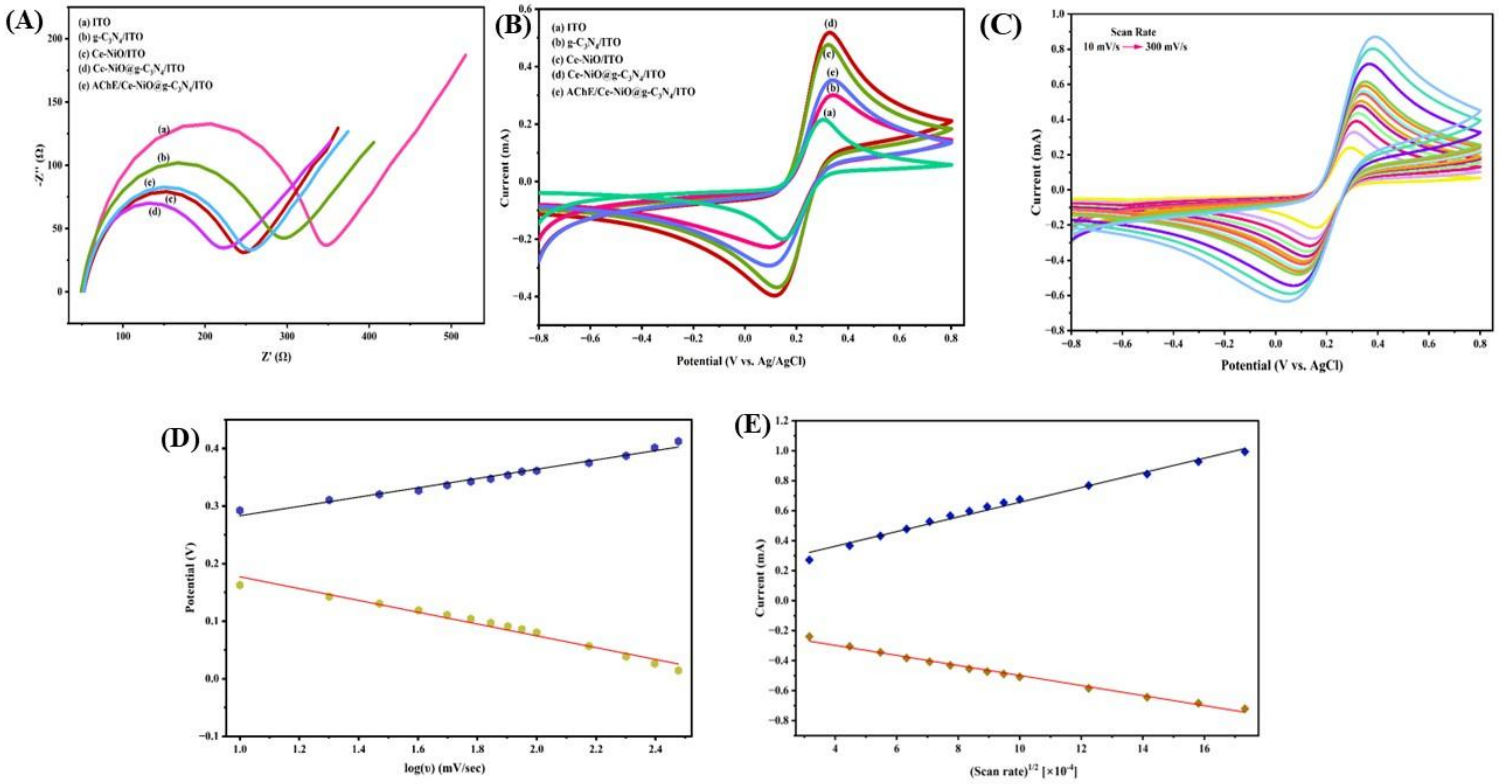

Fig. 4.4 (A) EIS study plot; **(B)** Cyclic voltammogram for different developed electrodes **(a)** ITO; **(b)** g-C_3N_4/ITO; **(c)** Ce-NiO/ITO; **(d)** Ce-NiO@g-C_3N_4/ITO and **(e)** AChE/Ce-NiO@g-C_3N_4/ITO; **(C)** Different scan rate of Ce-NiO@g-C_3N_4/ITO electrode (10-300 mV/sec); **(D)** Graph of current v/s square root of scan rate of Ce-NiO@g-C_3N_4/ITO; **(E)** Graph for potential v/s log (scan rate) of Ce-NiO@g-C_3N_4/ITO

The slopes obtained from the above equations were used to determine the electron transfer coefficient (α) and the electron transfer rate constant (K_s) for Ce-NiO@g-C_3N_4/ITO. The value of α was calculated to be 0.9236, and the corresponding K_s value was found to be 0.0969 s^{-1}. Furthermore, the anodic and cathodic peak currents (I_{pa} and I_{pc}) exhibited a linear relationship with the square root of the scan rate ($v^{1/2}$) for Ce-NiO@g-C_3N_4 /ITO **(Fig. 4.4 (E))**, as represented by the

following equations.

I_{pa} [Ce-NiO@g−C_3N_4/ITO] = 48.978μA (mV⁄s)$^{1/2}$ ×$v^{1/2}$ mV$s^{1/2}$+166.99μA; R^2 = 0.9890 **4.5**

I_{pc} [Ce-NiO@g−C_3N_4/ITO] = −33.489μA (mV⁄s)$^{1/2}$ ×$v^{1/2}$ mV$s^{1/2}$−163.72 μA; R^2=0.9912 **4.6**

Using the Randles–Sevcik equation (I_p=2.69×10^5 $n^{3/2}ACD^{1/2}v^{1/2}$), the effective surface area and diffusion coefficient were calculated to be 0.32 cm^2 and 12.828 × 10^{-6} cm^2 s^{-1}, respectively. Here, n denotes the number of electrons, C is the concentration of $[Fe(CN)_6]^{3-/4-}$ (mol cm^{-3}), and ν represents the scan rate (V s^{-1}).

4.3.4 Optimization Studies

The performance of the developed biosensor was optimized by tuning key parameters such as electrolyte pH, AChE concentration, and the pesticide inhibition period using DPV. The enzyme concentration was initially optimized within the range of 0.02–0.10 mg/mL in the presence of 2 mM ATCl, where the maximum current response was observed at 0.08 mg/mL **(Fig. 4.5 (A))**, indicating the optimal catalytic activity of AChE toward ATCl hydrolysis.

The effect of pH (6–8) on the sensor response showed that the highest current was observed at pH 7 (Fig. 4.5**B)**, which was selected for subsequent studies.

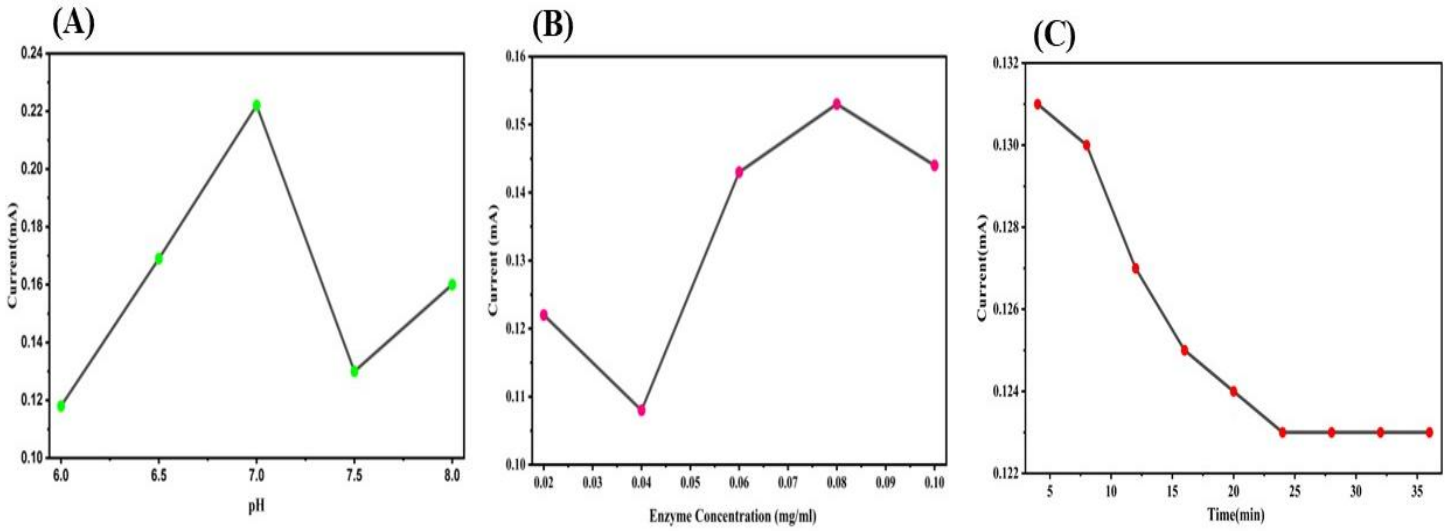

Fig. 4.5 Optimization studies of **(A)** AChE concentration, **(B)** Impact of pH of electrolyte, **(C)** Incubation time

Furthermore, as illustrated in **Fig. 4.5 (C)**, the incubation time study showed that the current starts decreasing with increasing time and stabilizes around 8 min when the duration is varied from 2 to 14 min, indicating optimal interaction between TF and AChE. Overall, these optimized conditions ensured enhanced sensitivity and reliable performance of the biosensor.

4.3.5 Electrochemical Biosensing Study

The electrochemical biosensing response of the fabricated AChE/Ce-NiO@g-C_3N_4/ITO electrode was investigated as a function of TF concentration (0.1 pM to 1 µM) in 0.2 M PBS (pH 7) containing 5 mM $[Fe(CN)_6]^{3-/4-}$ using the differential pulse voltammetry (DPV) technique. As shown in **Fig. 4.6 (A),** the anodic peak current decreases steadily with an increase in TF concentration. This decline in peak current is attributed to TF's inhibitory effect on AChE activity. **Fig. 4.6 (B)** presents the calibration curve, demonstrating a linear relationship between the peak current (I) and TF concentration, which follows the equation given below:

$$I=0.171\ \mu A/nM+3.379\mu A\times CTF;\ R_2=0.9796.$$

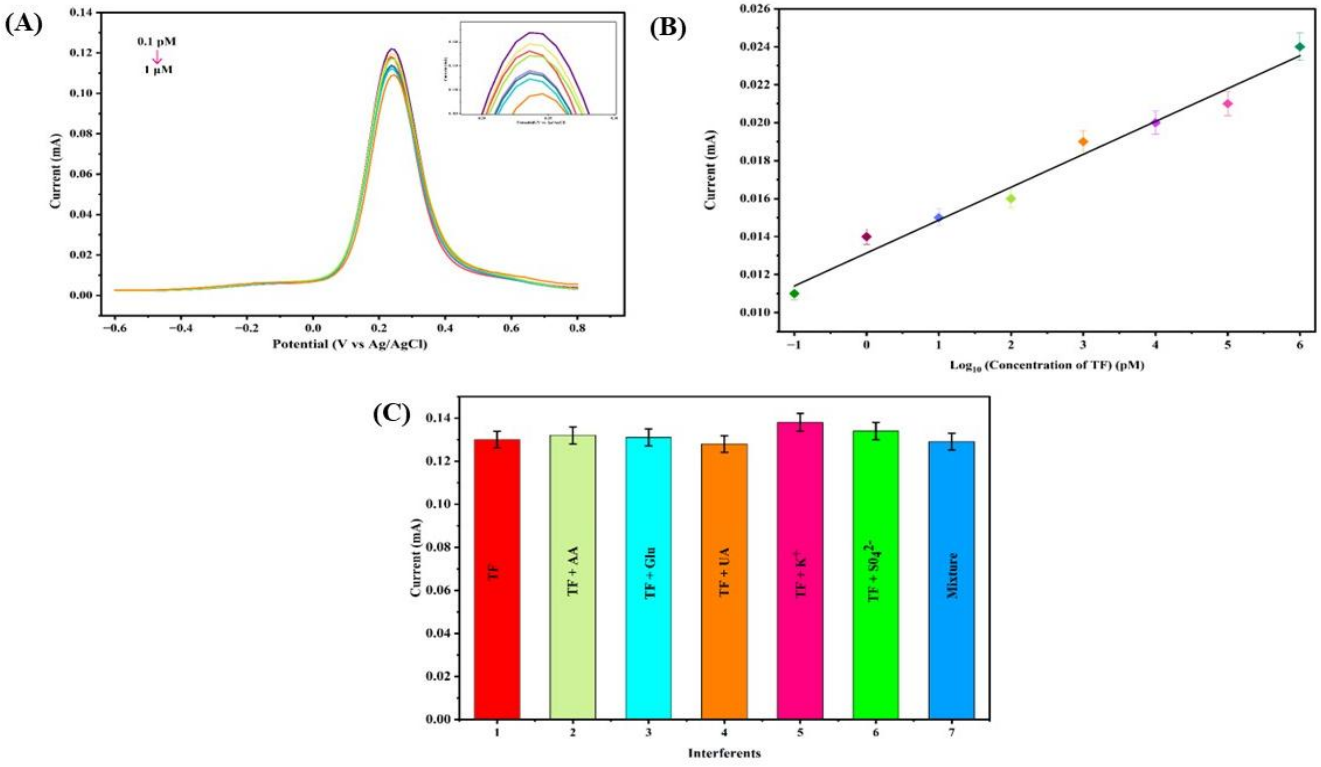

Fig. 4.6 (A) DPV response study of AChE/Ce-NiO@g-C_3N_4/ITO developed electrode at different concentrations of TF (0.1 pM to 1 µM); **(B)** Linearity plot for current v/s TF concentration; **(C)** Study of selectivity of AChE/Ce-NiO@g-C_3N_4/ITO electrode

The sensitivity of the proposed biosensor was calculated from the slope of the linear calibration plot (slope/effective surface area) and was found to be 0.51 μA $(pM)^{-1}$ cm^{-2}. The limit of detection (LOD) was determined to be 0.16 pM using the 3σ/S equation, where σ represents the standard deviation, and S denotes the sensitivity of the bioelectrode.

4.3.6 Interference Study and Real Sample Analysis

The selectivity performance of the AChE/Ce-NiO@g-C_3N_4/ITO biosensor was evaluated using a few interfering species, such as glucose, ascorbic acid, uric acid, K^+, and SO_4^{2-}. A mixture containing 1 pM interferents and 0.01 pM TF was tested. **Fig. 4.6 (C)** shows no apparent change in current response when the biosensor produced was exposed to interfering analytes, confirming its high selectivity for TF detection. The practical applicability of the biosensor was further assessed using spiked real samples (cucumber, apple, and rice) at concentrations of 0.1, 1, 10 and 100 pM. The obtained recovery values ranged from 95% to 104.5%, indicating good accuracy and reliability for TF detection in real samples.

Table 4.1 Detection of TF in three real samples using AChE/Ce-NiO@g-C_3N_4/ITO electrode

Samples	Added amount (pm)	Found amount (pm)	Recovery (%)	RSD (%)
Cucumber	0.1	0.98	98.3	1.14
	1	0.95	95.96	2.90
	10	9.59	95.93	2.93
	100	96.69	96.69	2.37
Apple	0.1	0.09	96.06	2.83
	1	0.95	95.2	3.47

	10	9.75	97.52	1.77
	100	97.5	97.5	1.79
Rice	0.1	0.10	100.8	0.58
	1	1.00	100.8	0.59
	10	10.17	101.7	1.20
	100	104.46	104.46	3.08

4.3.7 Reproducibility, Stability and Repeatability Studies

The reproducibility and long-term stability of the AChE/Ce-NiO@g-C_3N_4/ITO biosensor toward ATCl were evaluated to assess its performance. Reproducibility was tested using four independently fabricated electrodes in the presence of 1 pM TF **(Fig. 4.7 (A))**. The obtained RSD value of 3.96% indicates excellent reproducibility. For stability analysis, the electrode was stored at 4°C under dry conditions, and its DPV response was measured every 8 days **(Fig. 4.7 B)**. No significant decrease in current was observed within the first 10 days, and 94% of the original response was retained after 30 days, demonstrating excellent stability.

The repeatability of the AChE/Ce–NiO@g-C_3N_4/ITO biosensor was evaluated through ten successive measurements under identical conditions **(Fig. 4.7 C)**. The consistent peak-current responses, with an RSD of 0.35% (n = 10), indicate excellent operational stability and reliable performance.

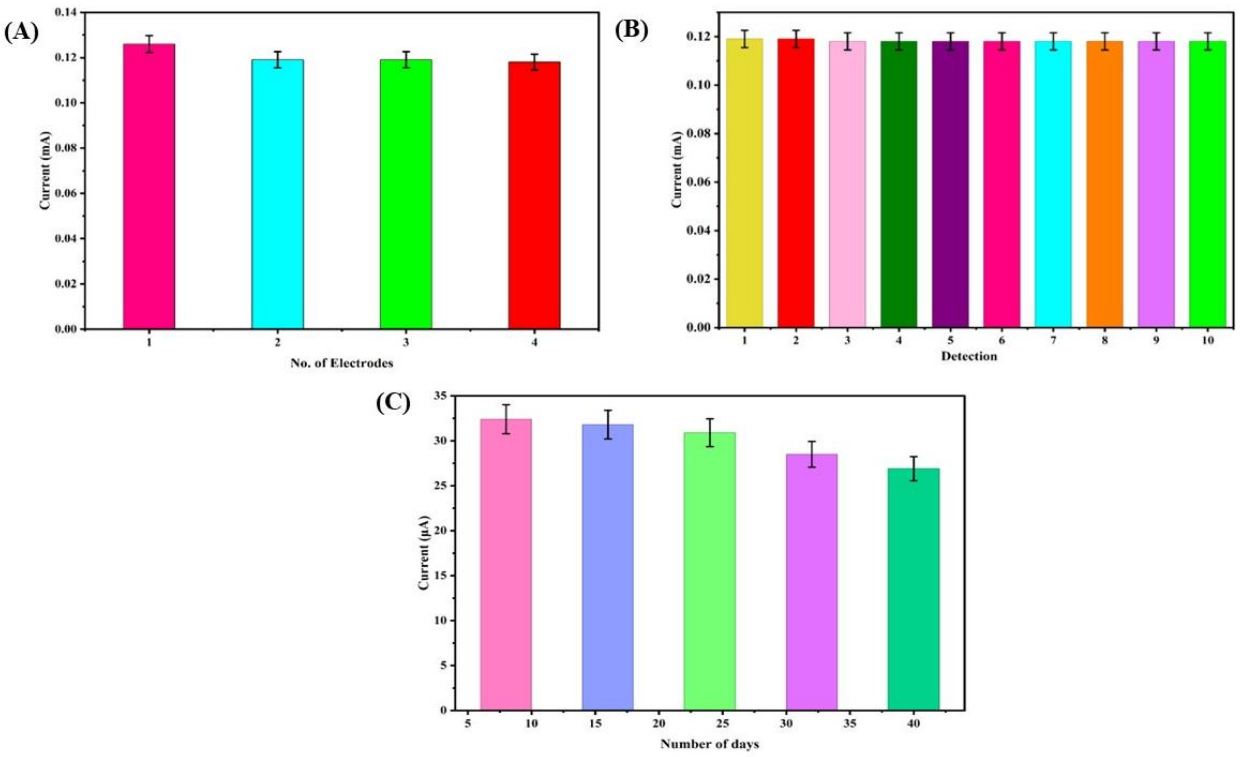

Fig. 4.7 (A) Reproducibility study of TF using different electrodes; **(B)** Stability study of the fabricated electrode (AChE/Ce–NiO@g-C_3N_4/ITO) over a period of 40 days; and **(C)** Repeatability study with the same electrode.

Chapter – 5

Conclusion

In summary, a novel AChE/Ce-NiO@g-C_3N_4-based electrochemical biosensor was successfully developed for the sensitive and selective detection of the organophosphate pesticide TF. The synergistic combination of Ce-NiO and g-C_3N_4 provided enhanced electron transfer, larger active surface area, superior biocompatibility, enabling efficient enzyme immobilization and improved sensing performance. After optimizing key experimental parameters such as the pH of PBS, the amount of enzyme AChE, and ATCl, and the incubation time, the fabricated biosensor exhibited high sensitivity (5.412 $\mu A \mu M^{-1} cm^{-2}$), a wide linear detection range (0.1 pM - 1 µM), a low detection limit of 0.1 pM, excellent reproducibility (RSD=3.06%, n=4), long-term stability, and strong anti-interference capability. Furthermore, the biosensor demonstrated satisfactory performance in analyzing real agricultural samples, including cucumber, apple, and rice, with excellent recovery values and low relative standard deviations. The outstanding analytical performance of the proposed sensor underscores the potential of the Ce-NiO@g-C_3N_4 nanocomposite as an advanced sensing material for pesticide monitoring. Owing to its simplicity, rapid response, cost-effectiveness, and reliability, the developed biosensor represents a promising platform for applications in food safety assessment, environmental monitoring, and agricultural quality control.

Conference Attended

Presented our work at the 3rd International Conference on Futuristic Material for Sustainable Development Goals-2026 (GMSDG 2026), organized by the Department of Chemistry, Chandigarh University, Gharuan, Punjab held on 09th – 10th April 2026.

CHANDIGARH UNIVERSITY
Discover. Learn. Empower.

QS UNIVERSITY RANKINGS 2026
INDIA'S NO. 1 PRIVATE UNIVERSITY

frontiers

ACS Chemistry for Life®

Department of Chemistry UIS

3RD INTERNATIONAL CONFERENCE ON

FUTURISTIC MATERIALS

FOR SUSTAINABLE DEVELOPMENT GOALS 2026

FMSDG 2026

CERTIFICATE

OF PARTICIPATION

This is to certify that Komal

from Delhi Technological University has participated & presented a Poster / Oral Paper entitled "Graphitic Carbon Nitride Functionalized Nickel-Cerium Bimetallic Oxide for Ultrasensitive Detection of Trichlorfon."

in the 3rd International Conference on Futuristic Materials for Sustainable Development Goals 2026 (FMSDG 2026) organised by the Department of Chemistry, University Institute of Sciences (UIS), Chandigarh University, Gharuan, Punjab, India, held on 09th–10th April 2026.

Their enthusiastic participation and contribution to the conference are sincerely appreciated.

Program Co-Chair
Prof. (Dr.) S. S. Chauhan
Director, UIS

Convener
Prof. (Dr.) Renu Sharma
Head, Department of Chemistry, UIS

Organising Secretary
Dr. Ruchi Bharti
Department of Chemistry, UIS


CHANDIGARH UNIVERSITY
Discover. Learn. Empower.
QS UNIVERSITY RANKINGS 2026
INDIA'S NO. 1
frontiers
ACS Chemistry for Life®
Department of Chemistry UIS
3RD INTERNATIONAL CONFERENCE ON
FUTURISTIC MATERIALS
FOR SUSTAINABLE DEVELOPMENT GOALS 2026
FMSDG 2026
CERTIFICATE
OF PARTICIPATION
This is to certify that Akanksha Katoch
from Delhi Technological University has participated & presented
a Poster / Oral Paper entitled "Graphitic Carbon Nitride Functionalized Nickel-Cerium Bimetallic Oxide for Ultrasensitive Detection of Trichlorfon."
in the 3rd International Conference on Futuristic Materials for Sustainable Development Goals 2026 (FMSDG 2026) organised by the Department of Chemistry, University Institute of Sciences (UIS), Chandigarh University, Gharuan, Punjab, India, held on 09th–10th April 2026.
Their enthusiastic participation and contribution to the conference are sincerely appreciated.
Program Co-Chair
Prof. (Dr.) S. S. Chauhan
Director, UIS
Convener
Prof. (Dr.) Renu Sharma
Head, Department of Chemistry, UIS
Organising Secretary
Dr. Ruchi Bharti
Department of Chemistry, UIS